Quantum Spintronics Design
(NV centers in diamond)

Eisuke Abe

RIKEN Center for Emergent Matter Science

2020.09.02

CMD Spintronics Design Course

(Online)

Short CV

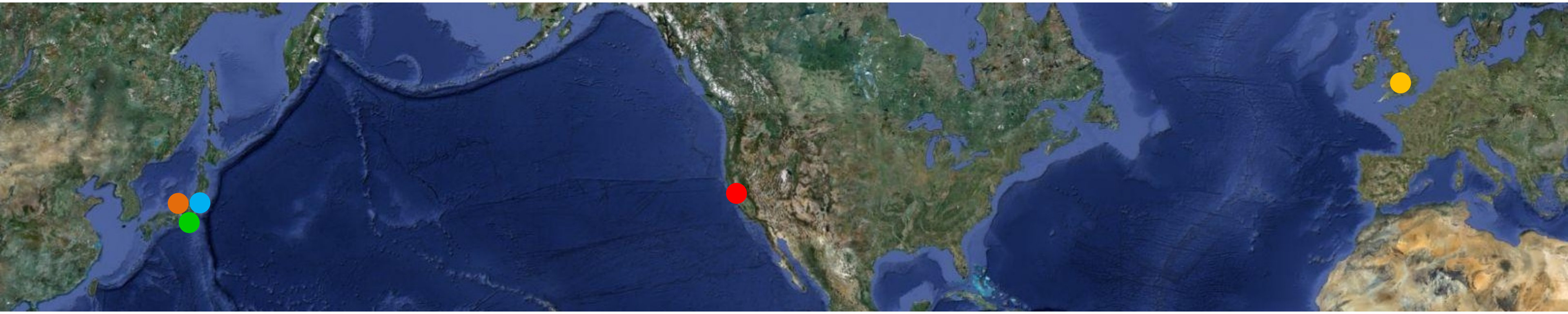

- **2001.4 – 2006.3 (Keio)** → Quantum computing (silicon)
- **2006.4 – 2009.12 (ISSP, UT)** → Quantum transport (GaAs QDs, Josephson)
- **2010.1 – 2011.6 (Oxford)** → Hybrid system (spin–cavity coupling)
- **2011.7 – 2015.3 (Stanford/RIKEN)** → Quantum network (InAs QDs)
- **2015.4 – 2019.1 (Keio)** → Quantum sensing (diamond)
- **2019.2 – Present (RIKEN)** → Quantum computing (Josephson)

Quantum technologies

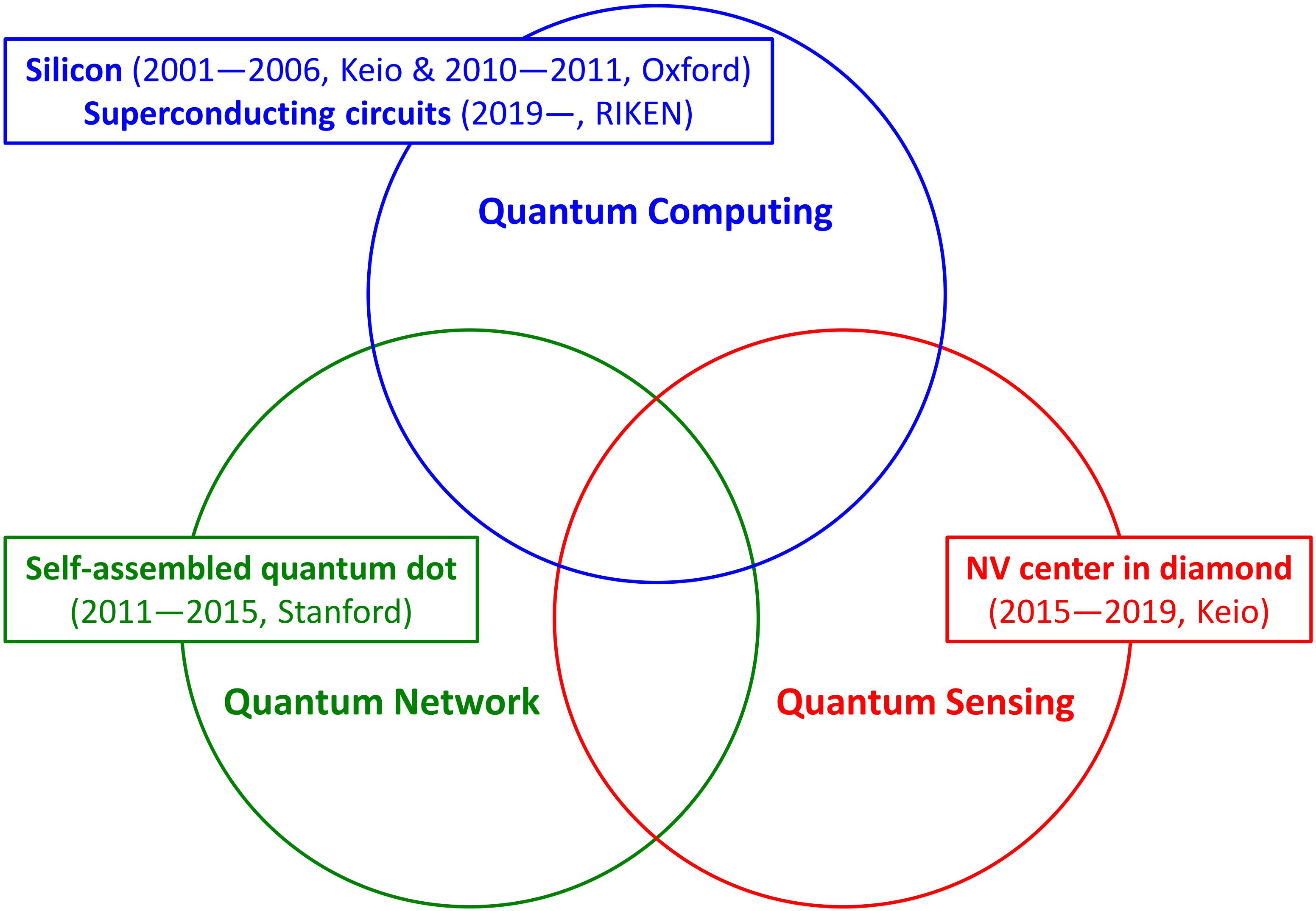

Quantum technologies

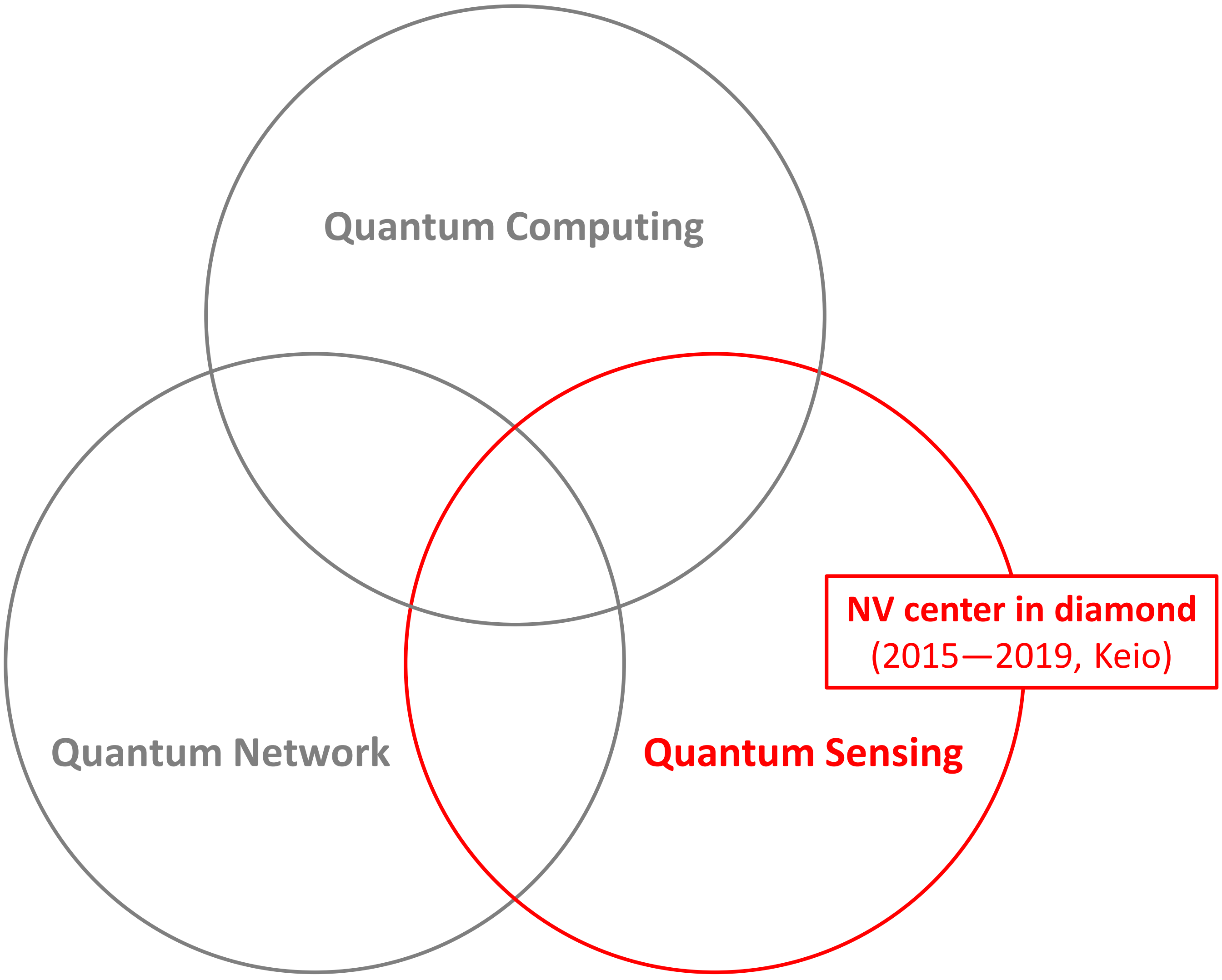

Outline

- **Basics of NV centers in diamond**
  - Structure
  - Optical properties
  - Spin properties and control
- **Quantum sensing**
  - DC magnetometry
  - AC magnetometry
  - Detection of proton spin ensemble
  - Ultrahigh resolution sensing

Outline

- **Basics of NV centers in diamond**
  - Structure
  - Optical properties
  - Spin properties and control

- **Quantum sensing**
  - DC magnetometry
  - AC magnetometry
  - Detection of proton spin ensemble
  - Ultrahigh resolution sensing

Diamond envy

©GIA

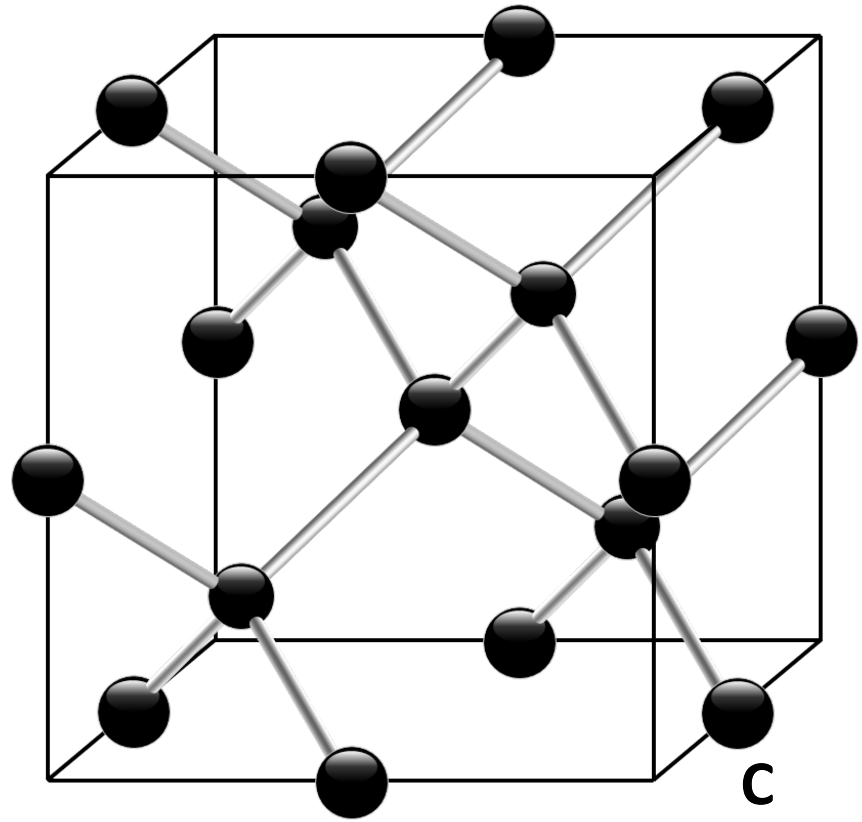

$\rho_N = 1.77 \times 10^{23}\ cm^{-3}$

Diamond NV

Synthetic (CVD) diamond
2^2 x 0.5 mm^3, $700 (E6)
[N] < 5 ppb, [NV] < 0.03 ppb

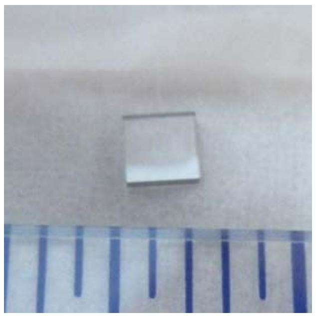

Not like…

©GIA

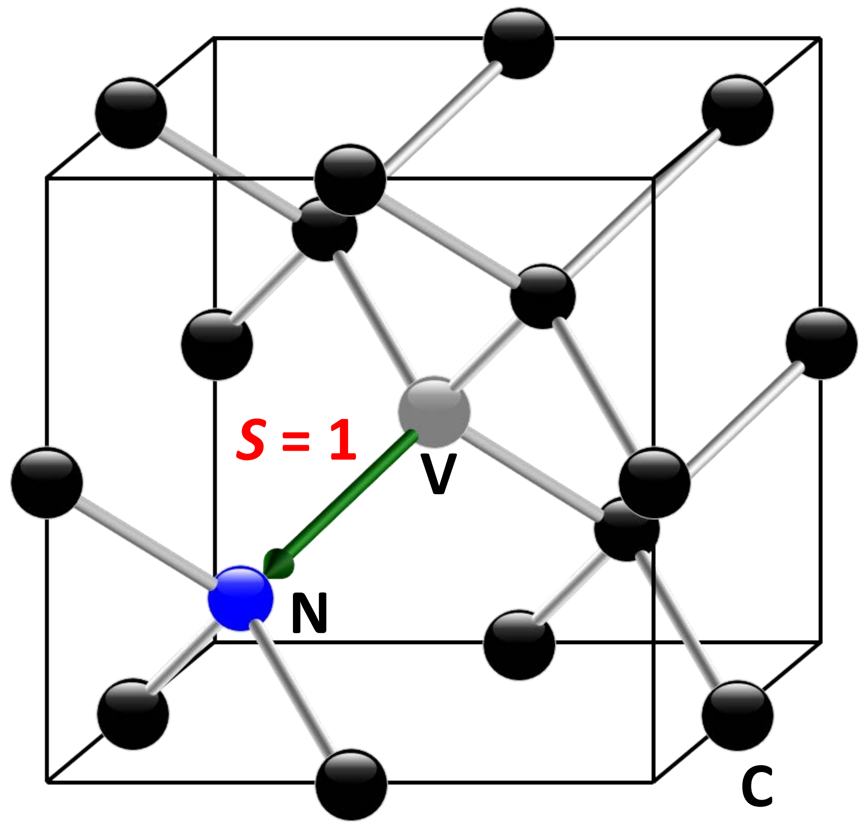

ρ_N = 1.77 x 10^{23} cm^{-3}

Crystal & energy level structures

- Negatively-charged (NV^-)
- 4 sp^3 orbitals, 6 e^- (5 from the defect, 1 captured)
- C_{3v} (symmetry axis = quantization axis)

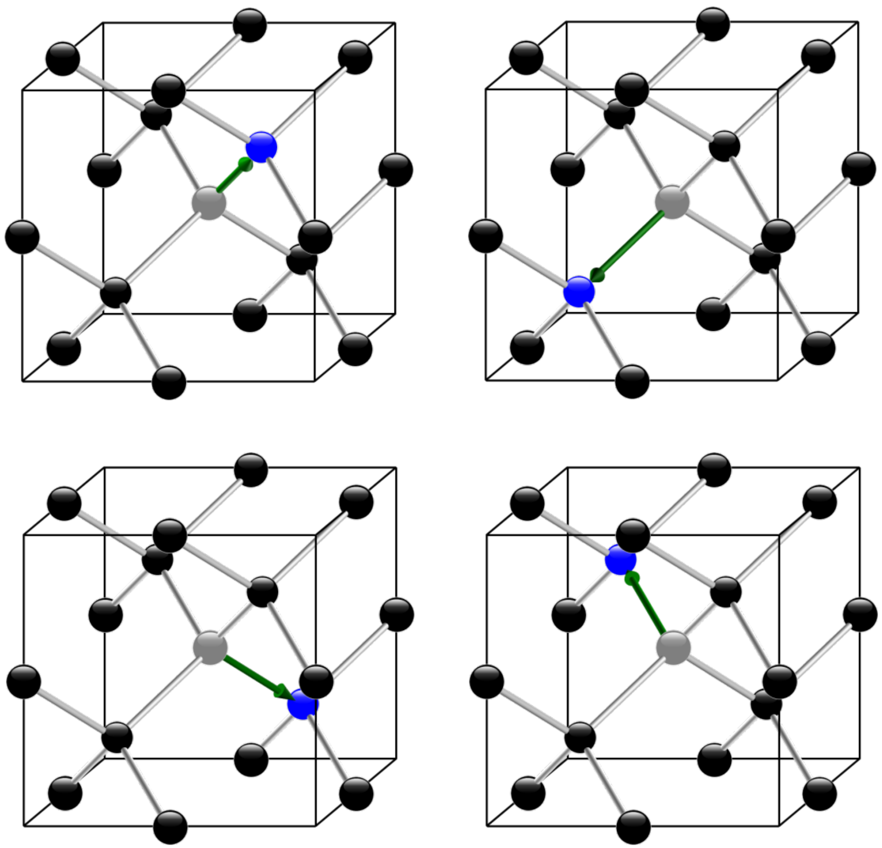

Effective spin-1 system
(e^2-hole spin-triplet)

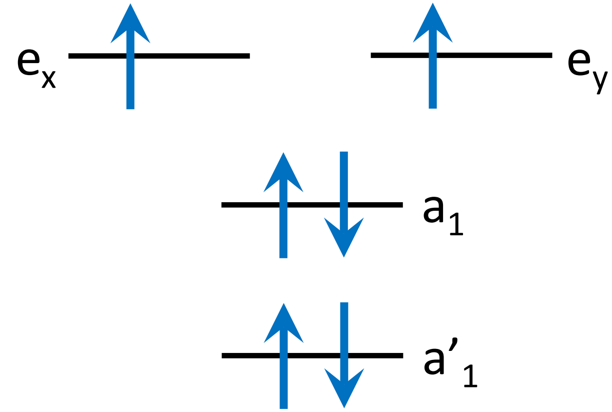

Energy levels

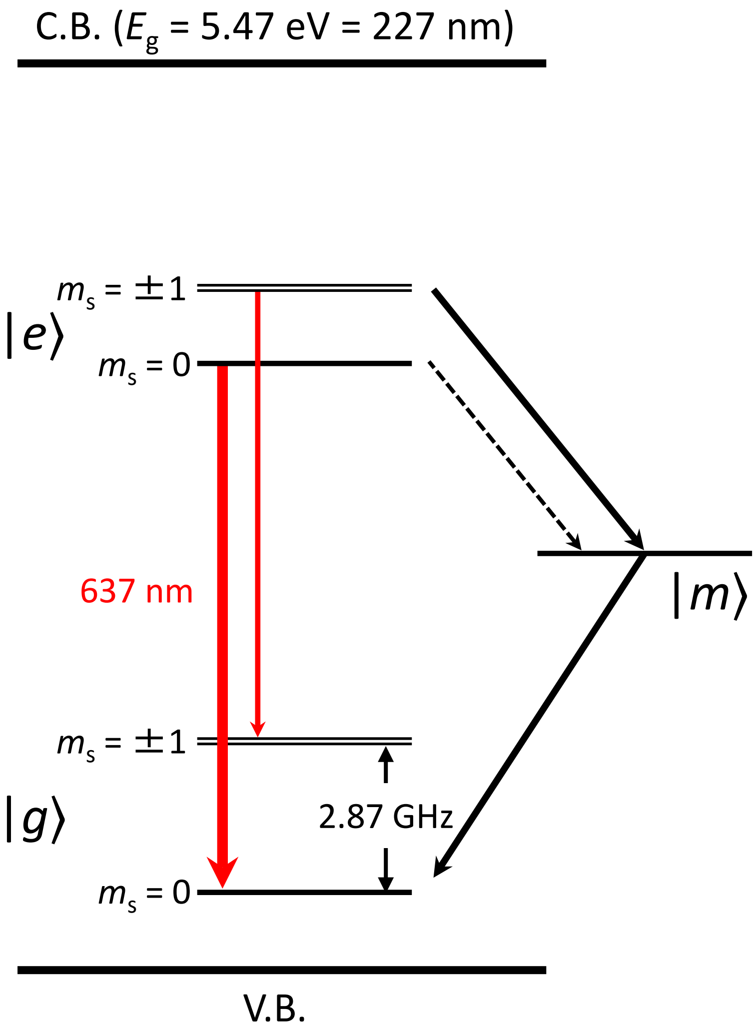

PL spectroscopy & imaging

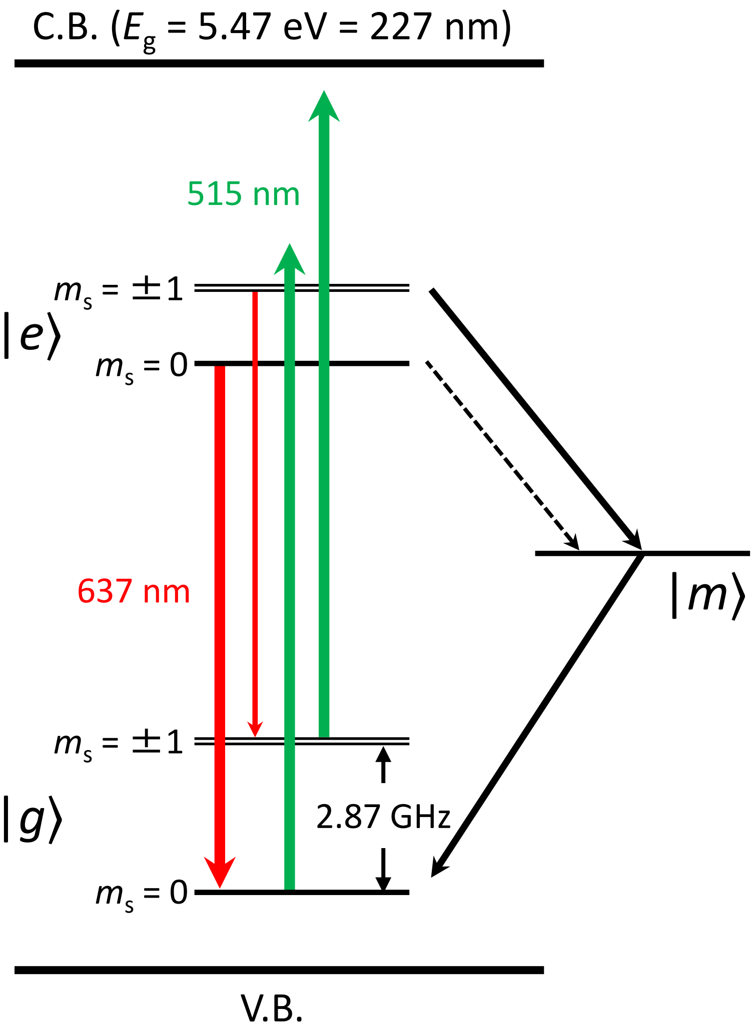

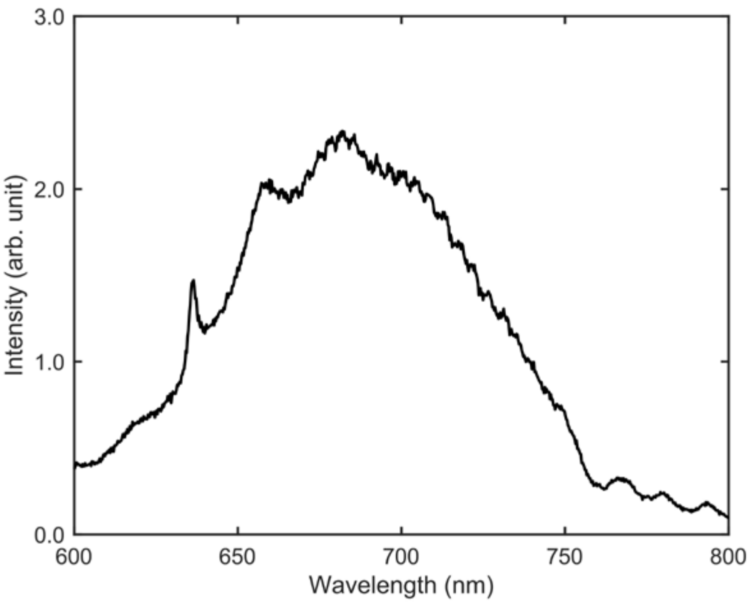

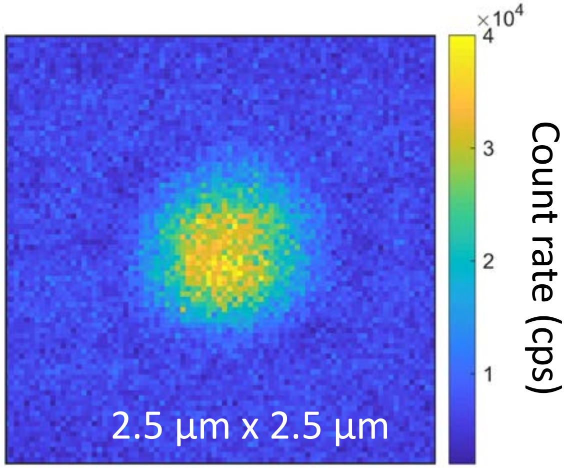

Photon statistics

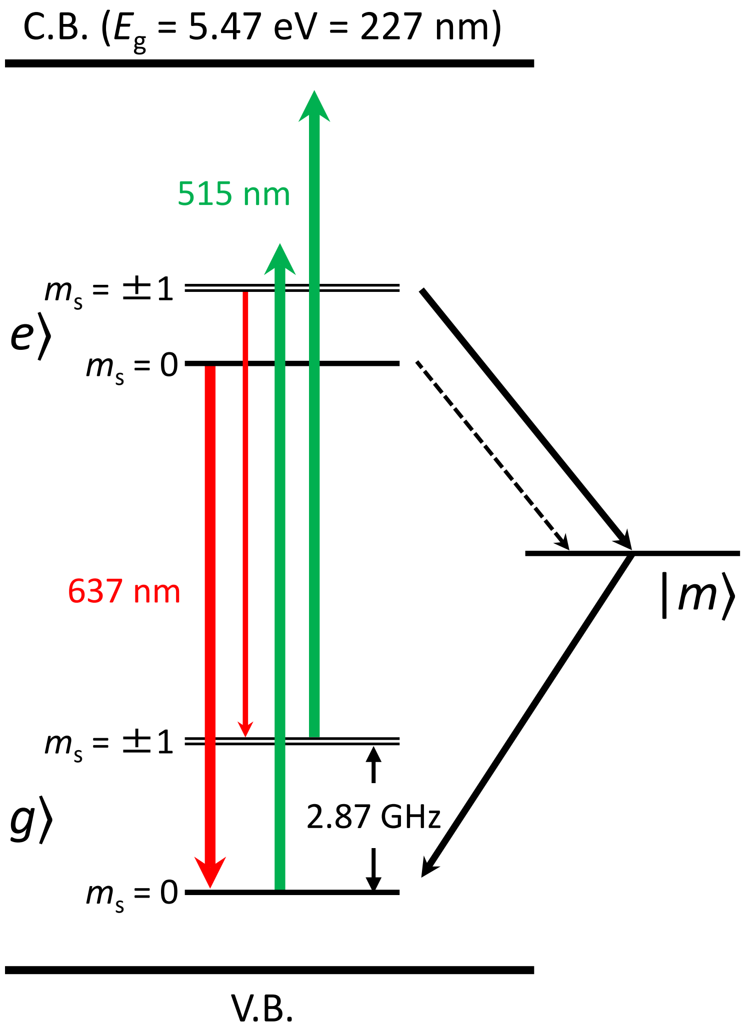

One photon at a time

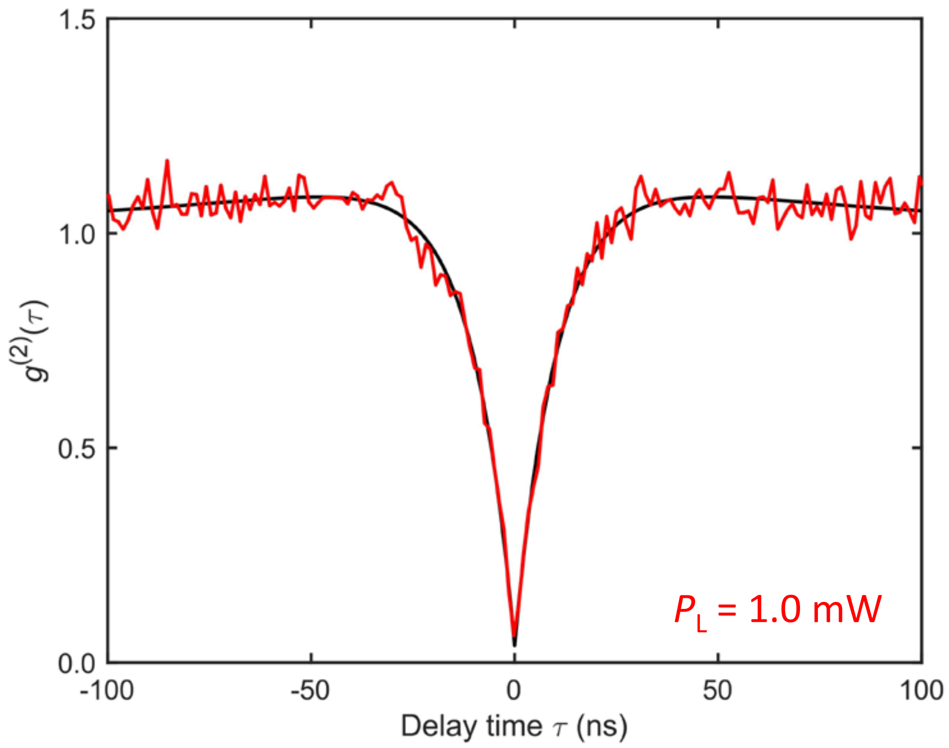

Time-resolved fluorescence

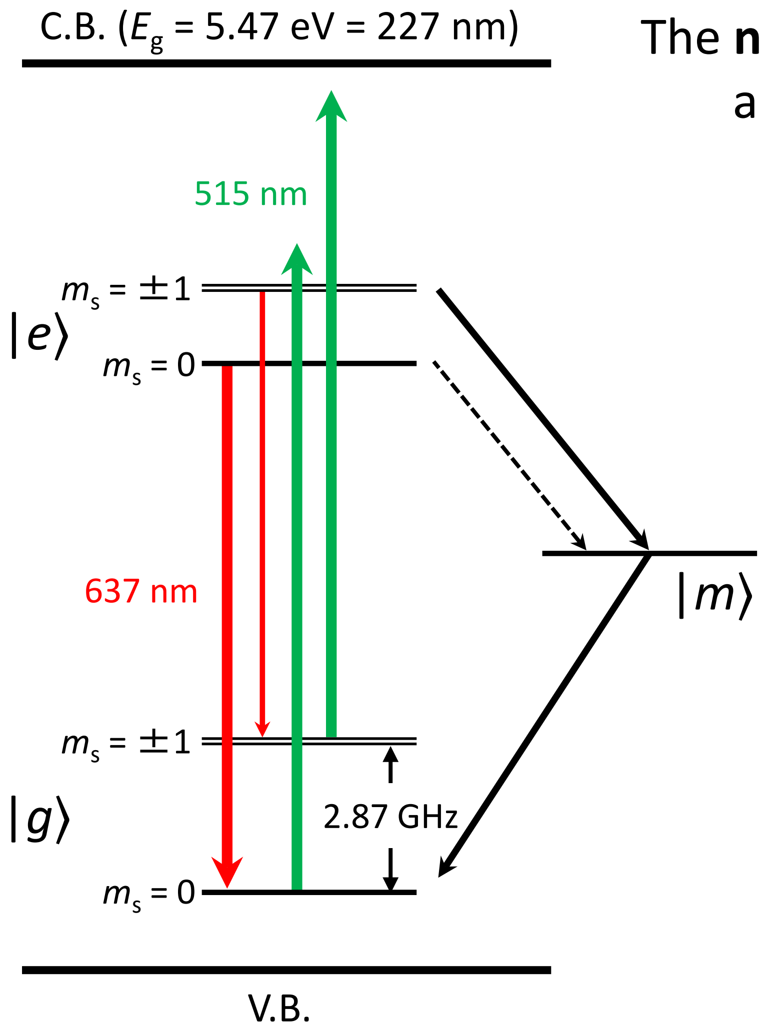

The **non-radiative** & **spin-selective** channel provides a means to **read out** & **initialize** the NV spin

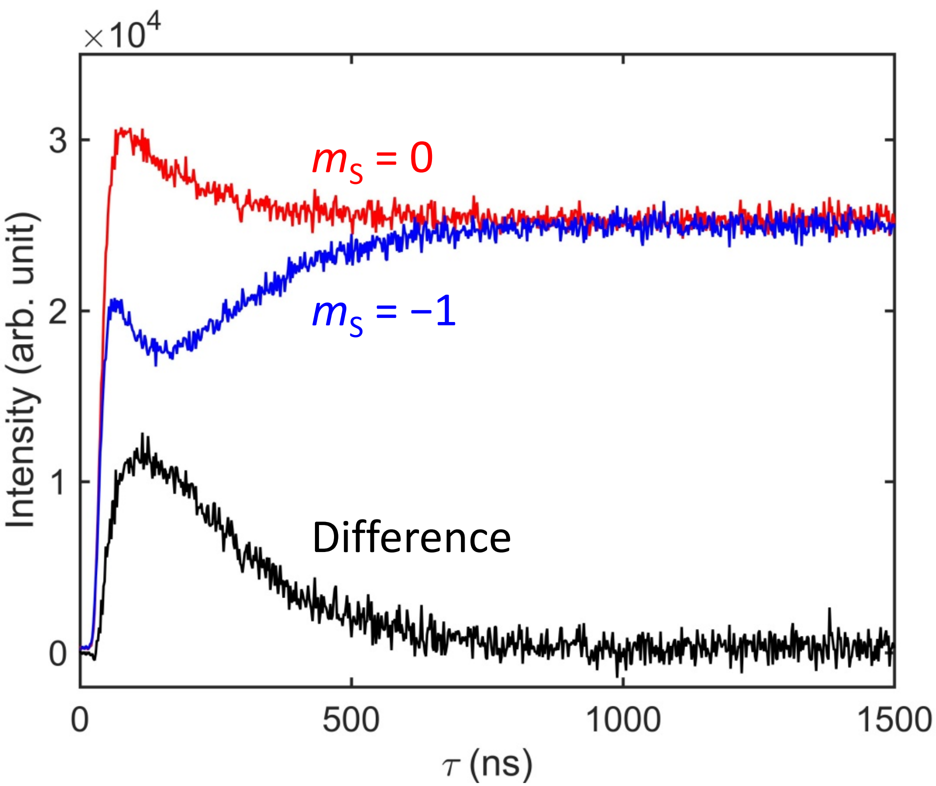

CW ODMR at $B_0 = 0$

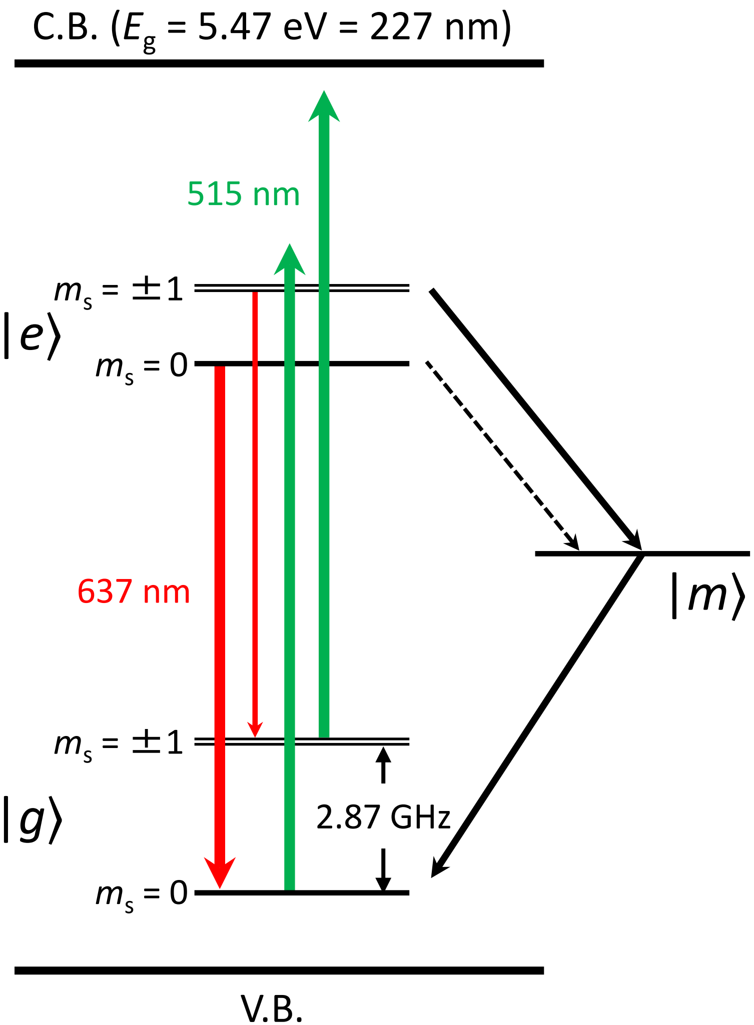

Zero-field splitting $H = DS_z^2$

D = 2.87 GHz

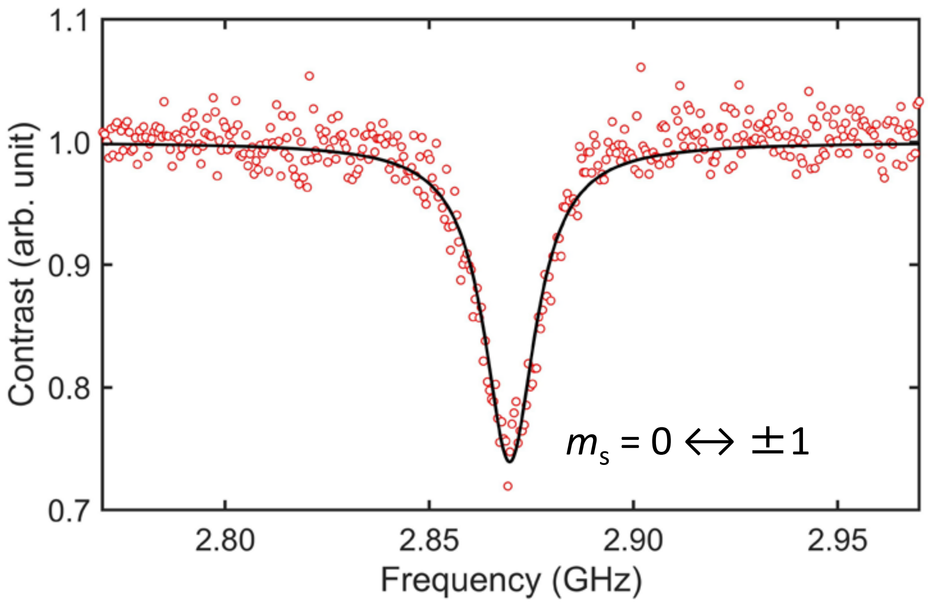

CW ODMR at $B_0 > 0$

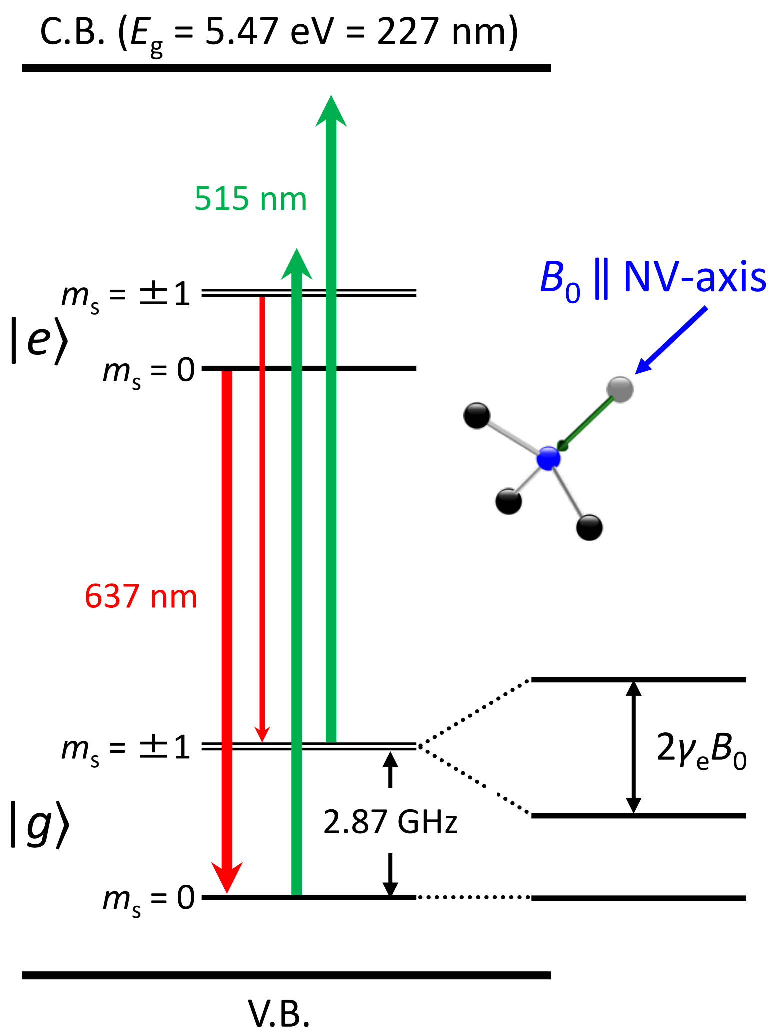

Zeeman $H = DS_z^2 + \gamma_e B_0 S_z$

γ_e = 28 MHz/mT

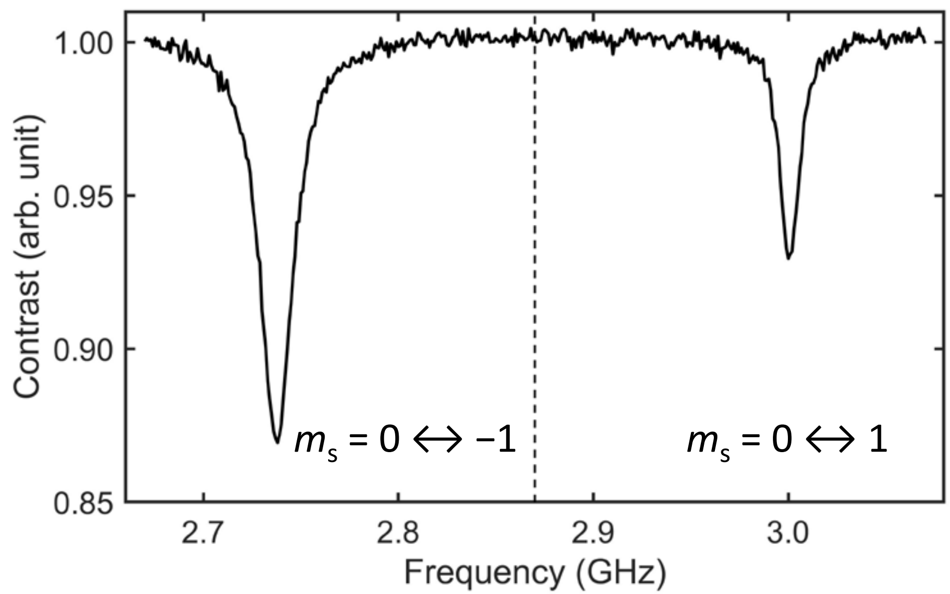

B_0 = 4.7 mT (2.87±0.132 GHz)

Experimental setup

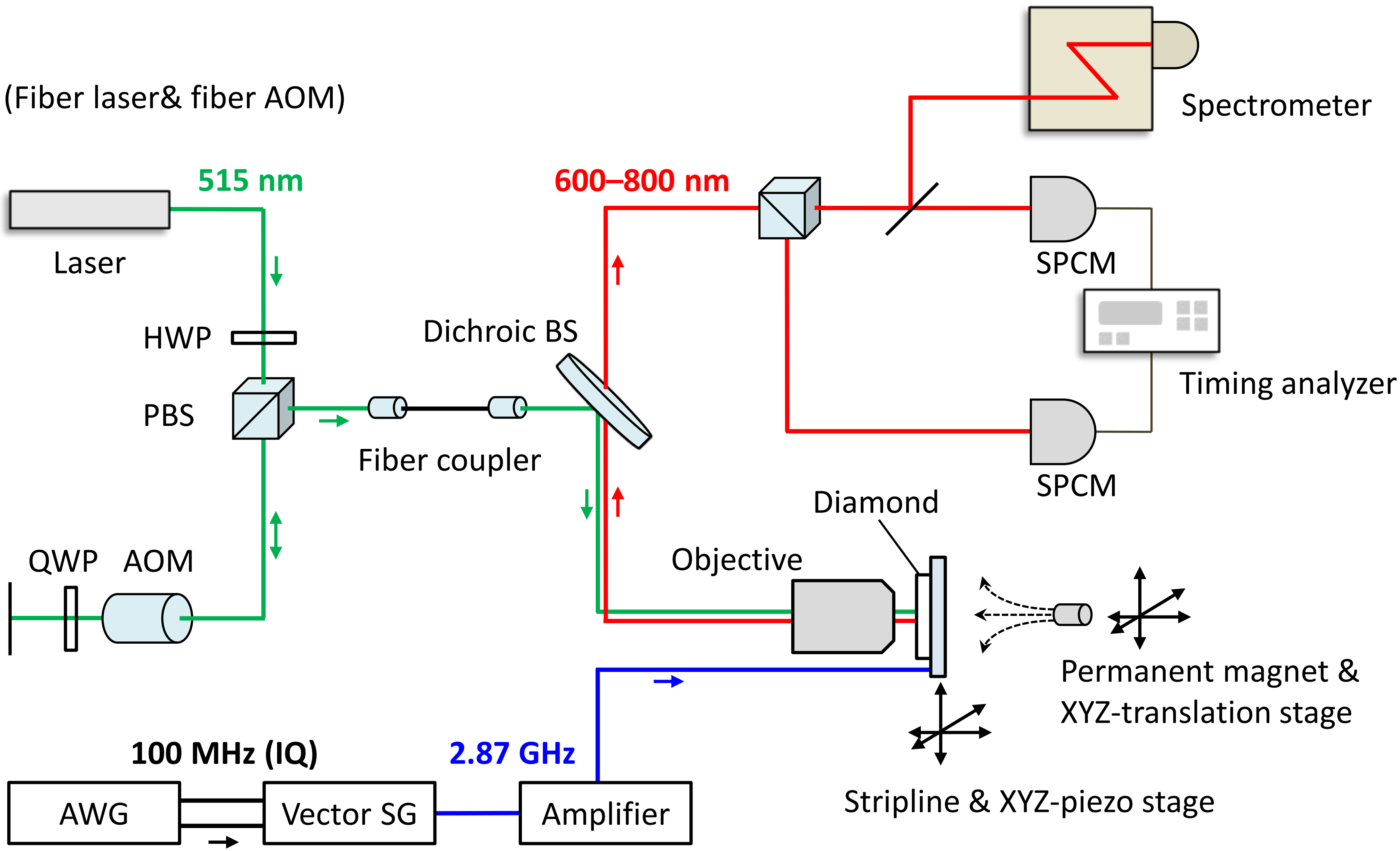

(XY-galvo + Z-piezo & 1-axis magnet)

Experimental setup

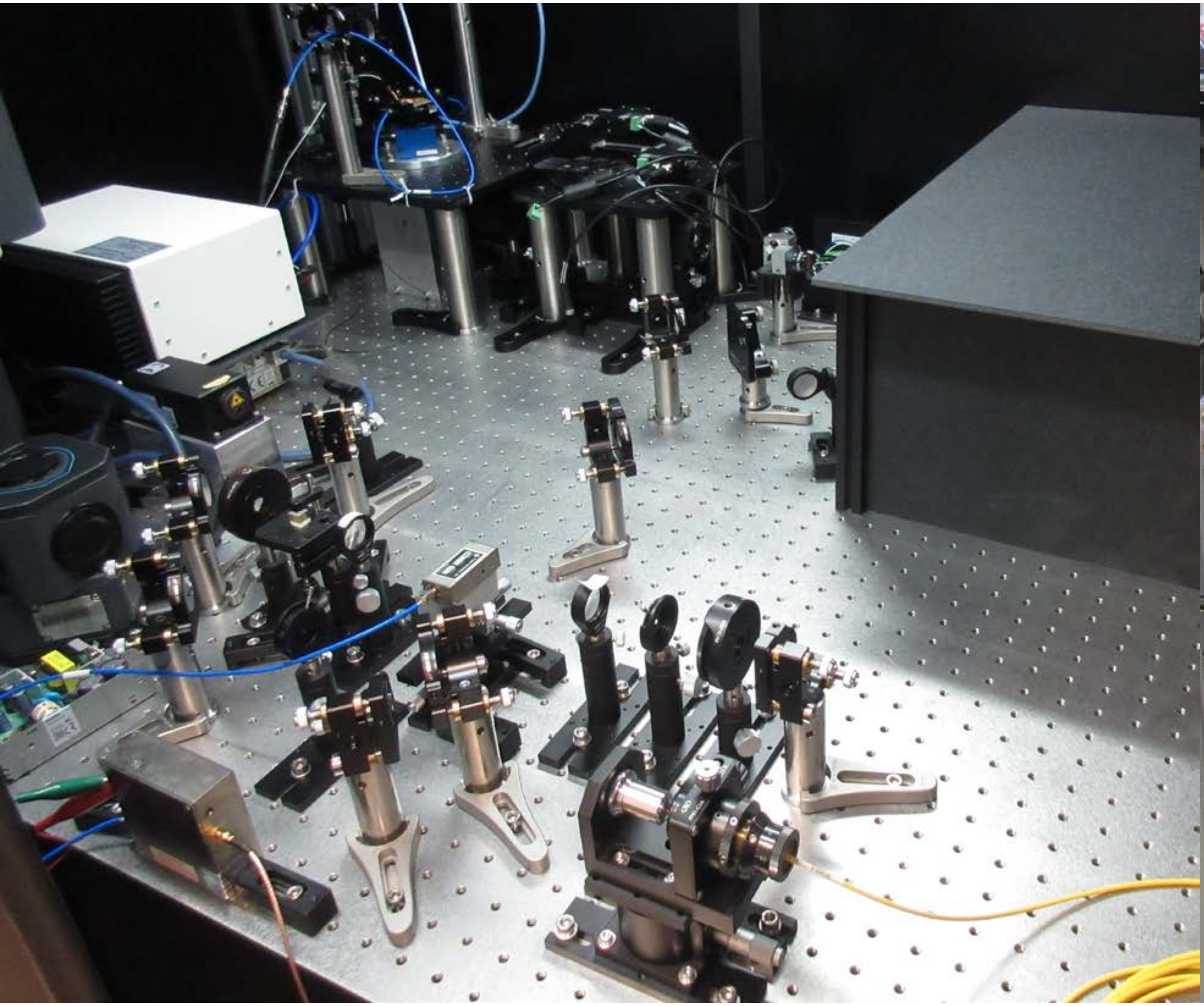

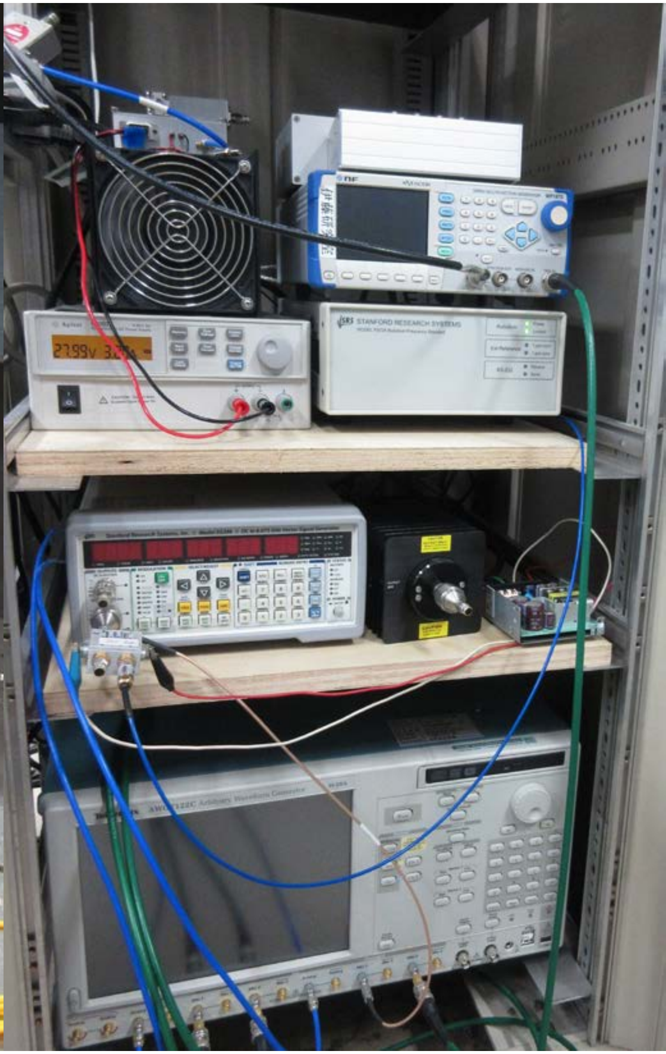

Experimental setup

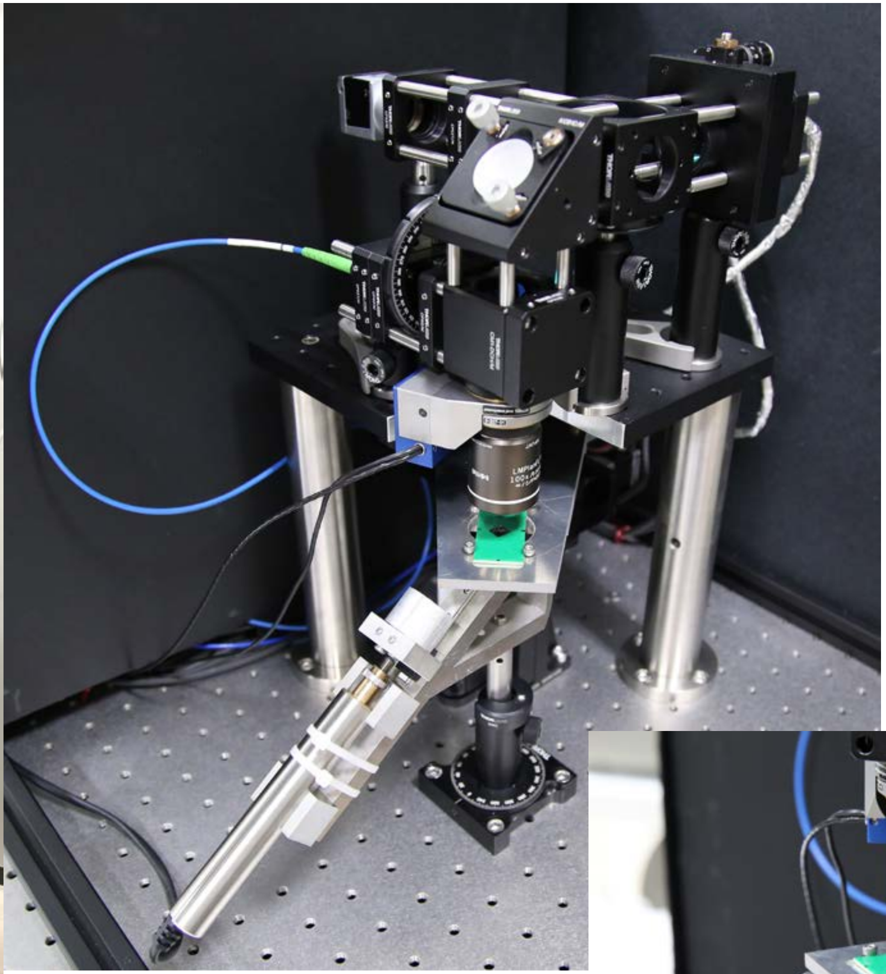

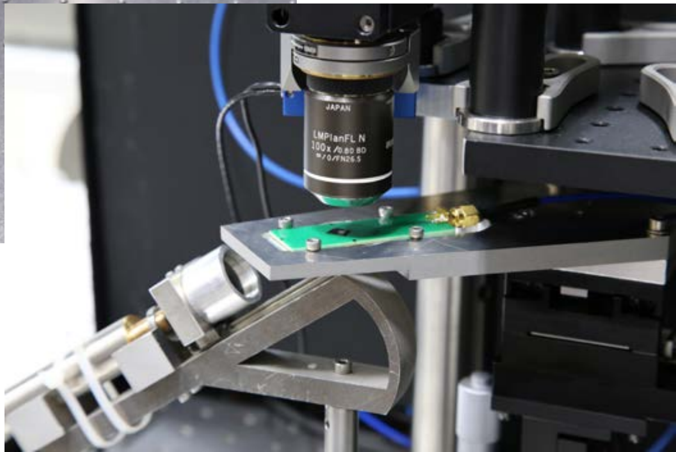

AIP Advances **10**, 025206 (2020)
Misonou *et al.*

Outline

- **Basics of NV centers in diamond**
  - Structure
  - Optical properties
  - Spin properties and control
- **Quantum sensing**
  - DC magnetometry
  - AC magnetometry
  - Detection of proton spin ensemble
  - Ultrahigh resolution sensing

Quantum sensing with NV centers

- *B*, *E*, *T*, *S*...
- DC & AC modes
- Wide temperature range
- Nondestructive
- High spatial resolution
- Various modalities

Nanodiamond & biology

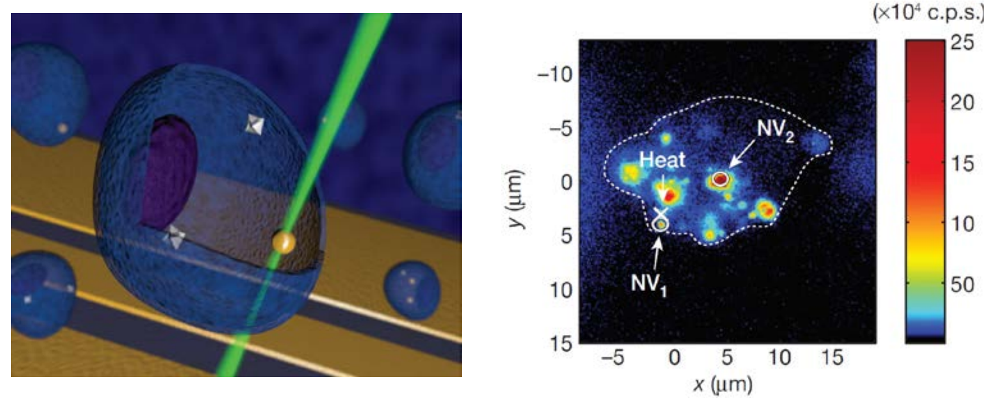

Nature **500**, 54 (2013)

Near-surface NV center & NMR

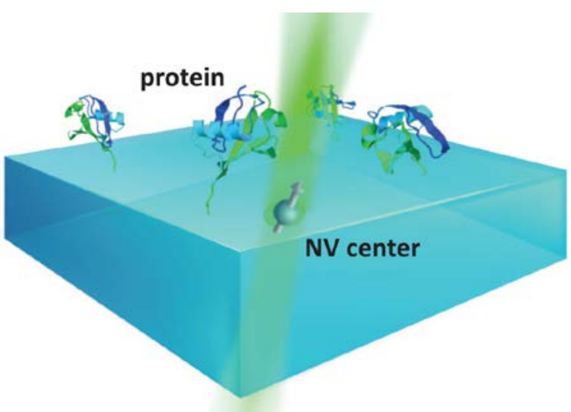

Science **351**, 836 (2016)

Scanning probe & condensed matter

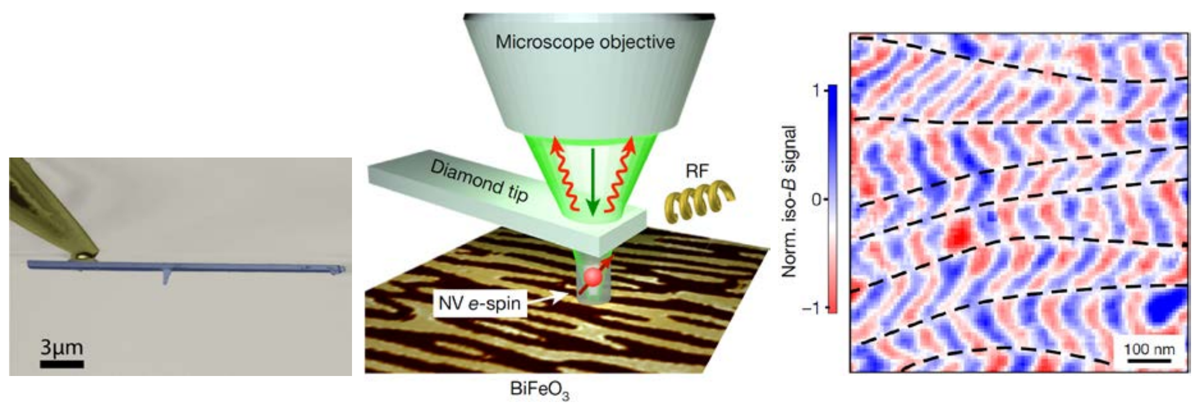

Rev. Sci. Instrum. **87**, 063703 (2016); Nature **549**, 252 (2017)

Outline

- **Basics of NV centers in diamond**
  - Structure
  - Optical properties
  - Spin properties and control
- **Quantum sensing**
  - DC magnetometry
  - AC magnetometry
  - Detection of proton spin ensemble
  - Ultrahigh resolution sensing

DC magnetometry

Single NV in bulk ($m_S = 0 \leftrightarrow -1$)

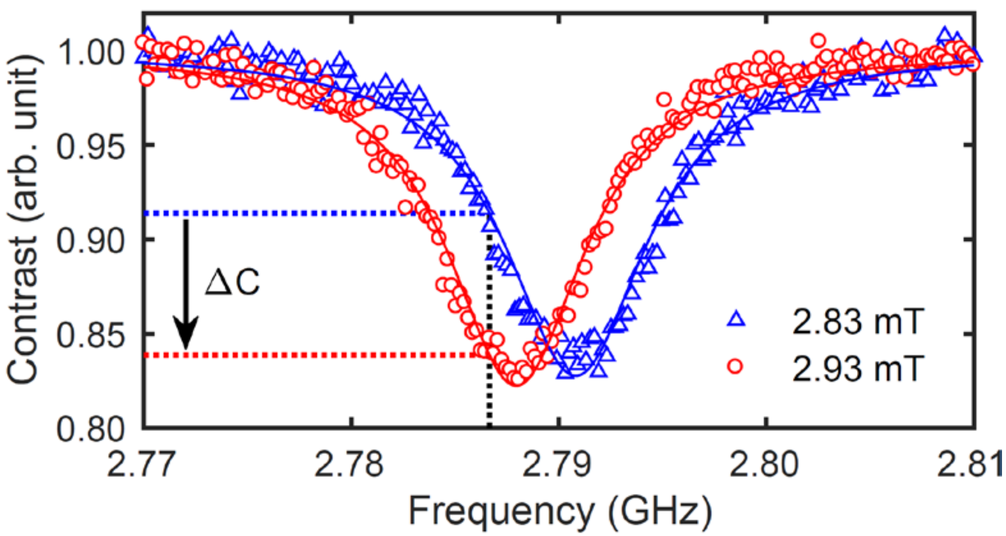

DC sensitivity

FWHM (MHz)

$$\eta_{sn}^{(cw)} = \frac{\delta\nu}{\gamma_e C \sqrt{I_0}}$$

Contrast (%)

Count rate (/s)

$$\frac{8.2\ \text{MHz}}{(0.18)(30\ \text{kcps})^{0.5}} \rightarrow 10\ \mu\text{T/Hz}^{0.5}$$

High sensitivity = Narrow *δν*, high *C*, high I_0

J. Appl. Phys. **123**, 161101 (2018) Abe & Sasaki

Vector magnetometry

Ensemble NV at the surface ($m_S = 0 \leftrightarrow \pm 1$)

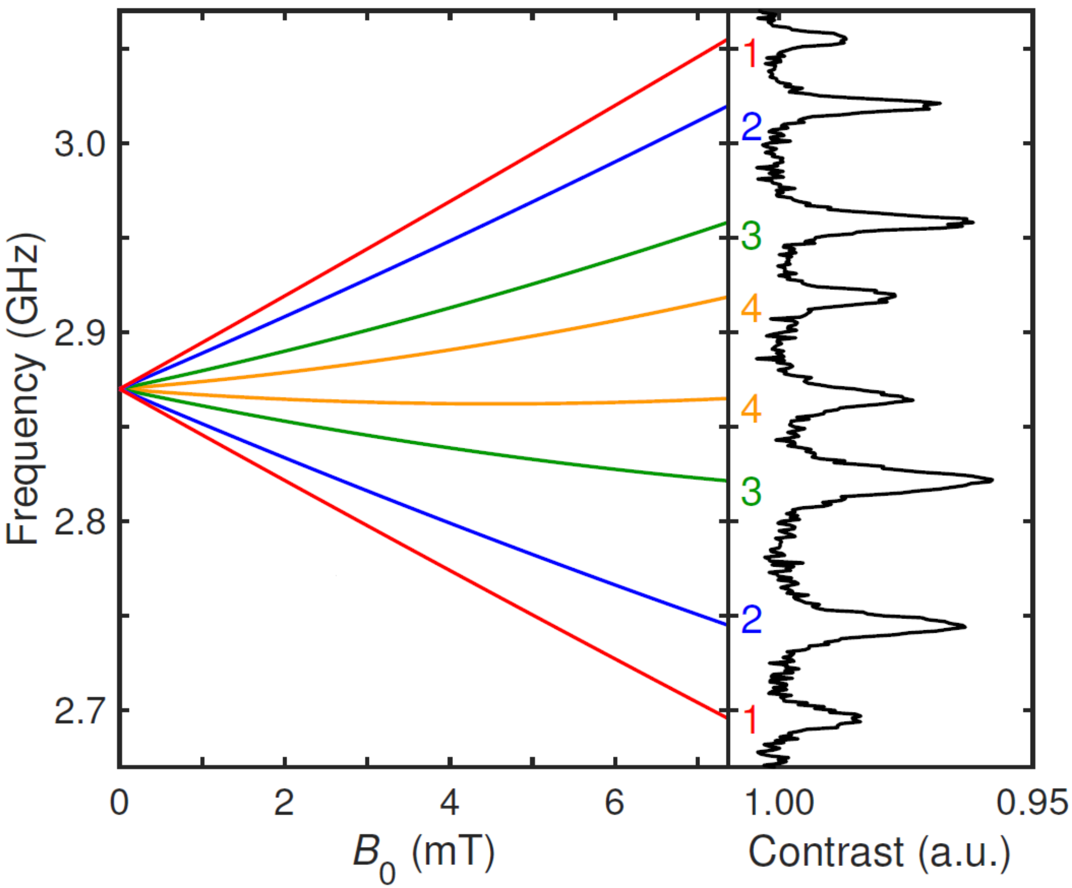

$$H^{(i)} = D\left(S_z^{(i)}\right)^2 + \gamma_e \boldsymbol{B}_0 \cdot \boldsymbol{S}^{(i)}$$
$$\approx D\left(S_z^{(i)}\right)^2 + \gamma_e B_0 \cos\beta_i \, S_z^{(i)}$$

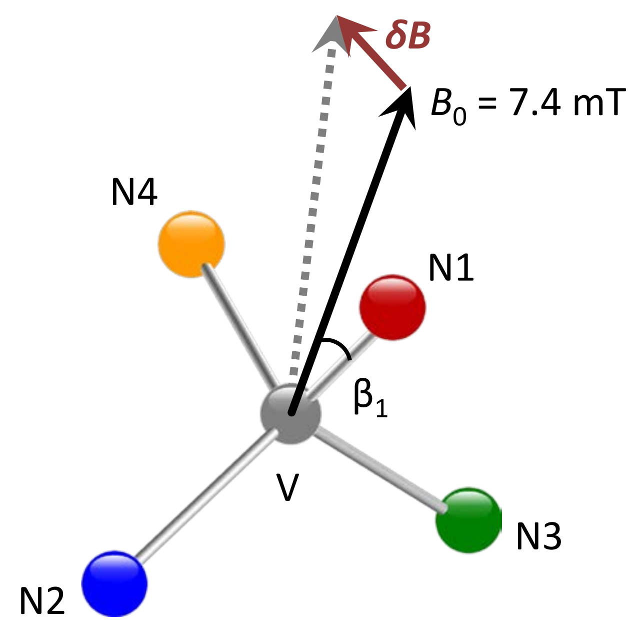

$\beta_1 = 29^o$, $\beta_2 = 132^o$, $\beta_3 = 109^o$, $\beta_4 = 83^o$

Rev. Sci. Instrum. **87**, 053904 (2016) Sasaki *et al.*

J. Appl. Phys. **123**, 161101 (2018) Abe & Sasaki

Magnetic imaging: Biology

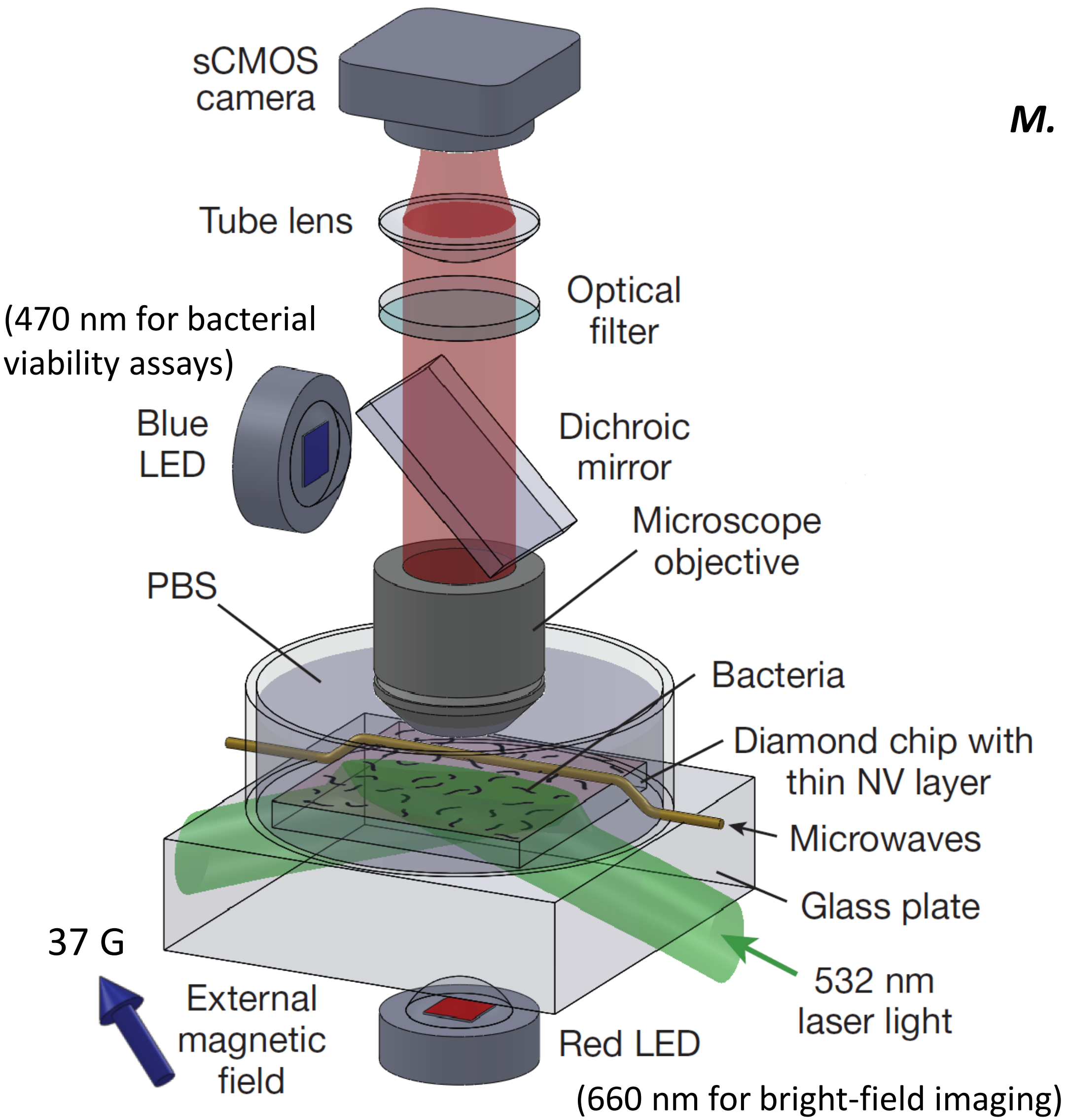

***M. magneticum* AMB-1 bacterium**

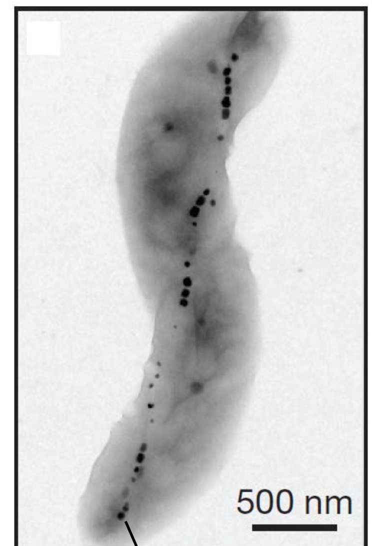

Magnetosome (Fe_3O_4 nanoparticle)

Nature **496**, 486 (2013) Le Sage *et al.*

Magnetic imaging: Biology

Magnetotactic bacteria (MTB) adhered to the diamond surface

(100 x 30 μm^2 area with 400 nm resolution)

Dried MTB

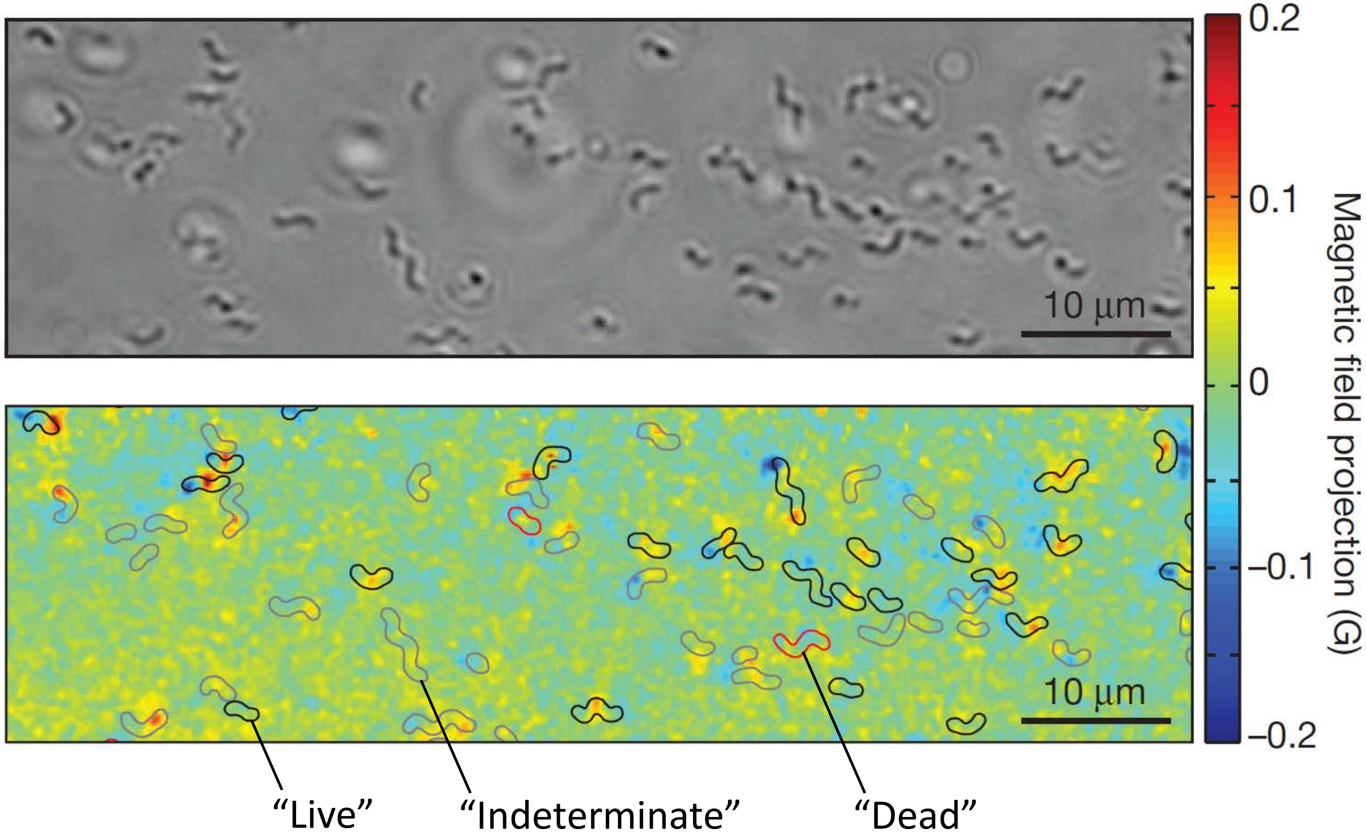

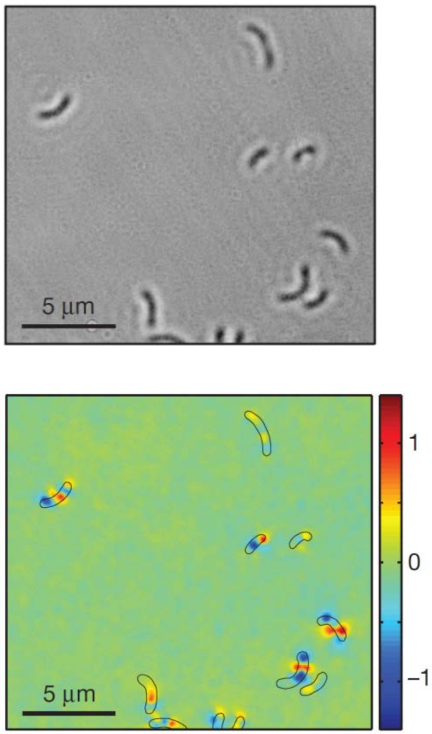

Nature **496**, 486 (2013) Le Sage *et al.*

Magnetic imaging: Biology

Measured

Simulated

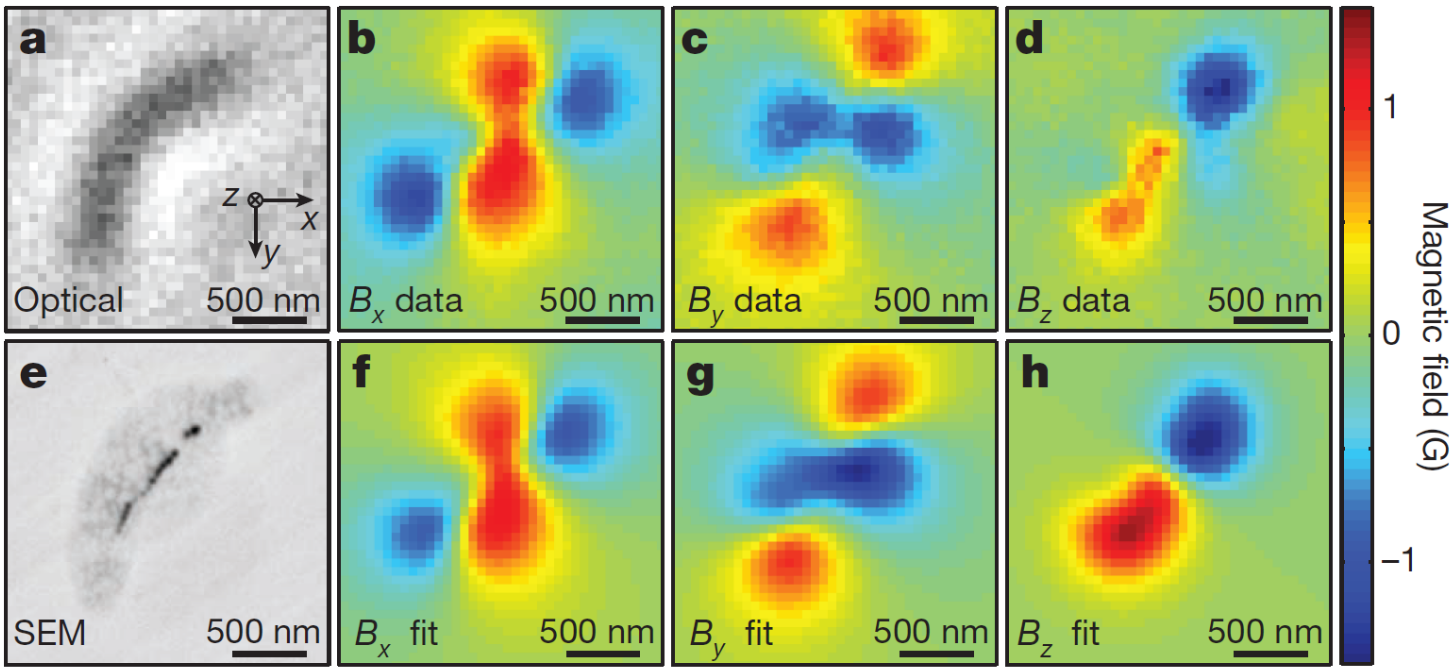

Vector plots

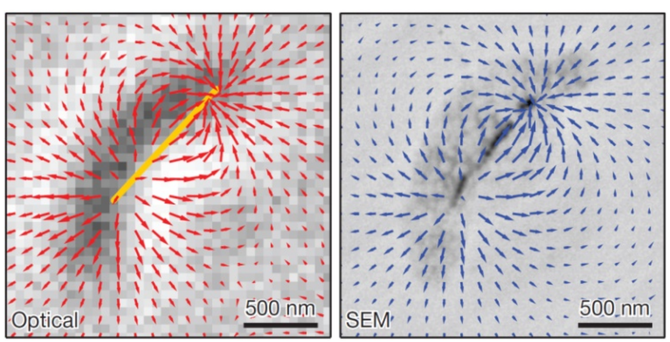

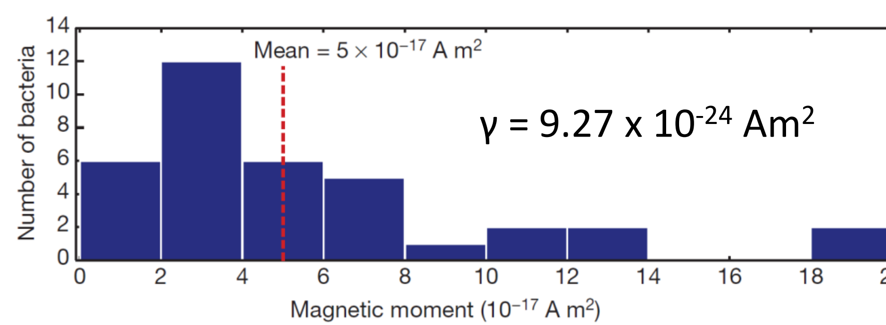

$\gamma = 9.27 \times 10^{-24}$ Am^2

Nature **496**, 486 (2013) Le Sage *et al.*

Magnetic imaging: Geoscience

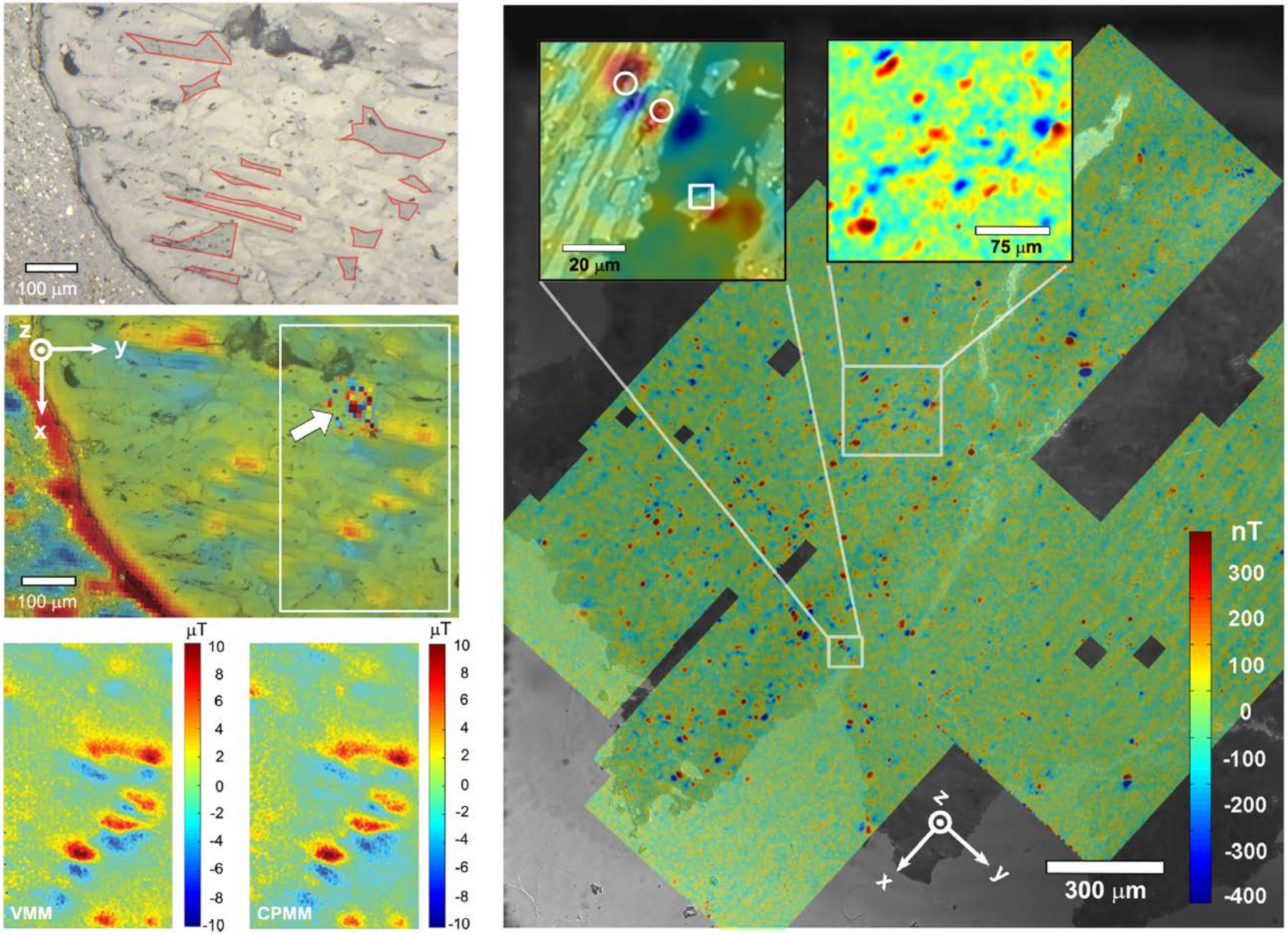

Geochem. Geophys. Geosyst. **18**, 3254 (2017) Glenn *et al.*

Magnetic imaging: Geoscience

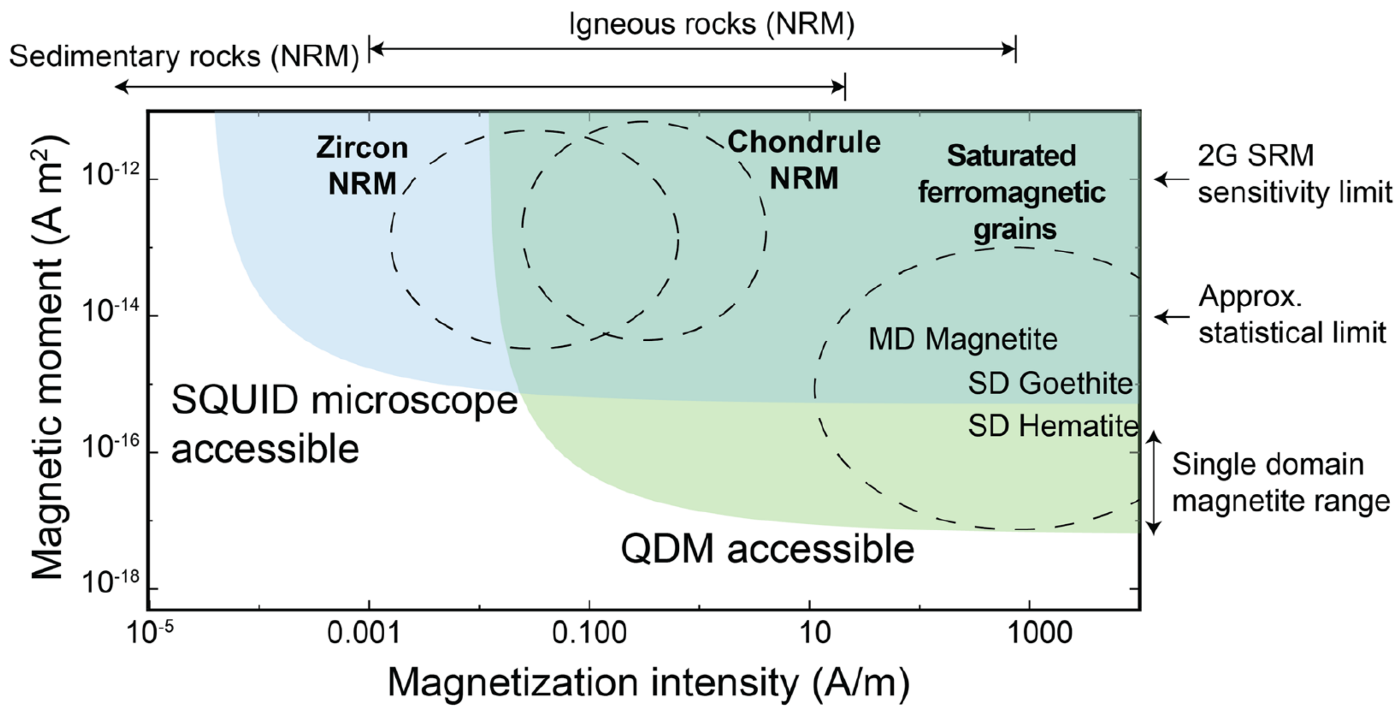

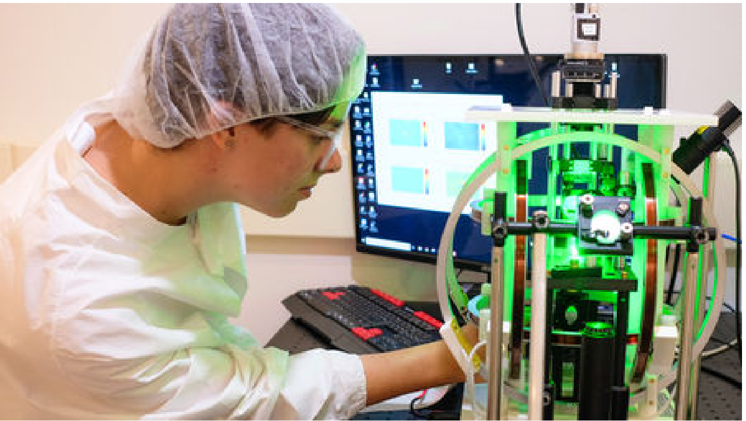

https://www.sciencemag.org/news/2020/04/diamond-microscope-reveals-slow-crawl-earth-s-ancient-crust

https://paleomag.fas.harvard.edu/

Geochem. Geophys. Geosyst. **21**, e2020GC009147 (2020) Fu *et al.*

Outline

- **Basics of NV centers in diamond**
  - Structure
  - Optical properties
  - Spin properties and control
- **Quantum sensing**
  - DC magnetometry
  - AC magnetometry
  - Detection of proton spin ensemble
  - Ultrahigh resolution sensing

Nuclear spin sensing

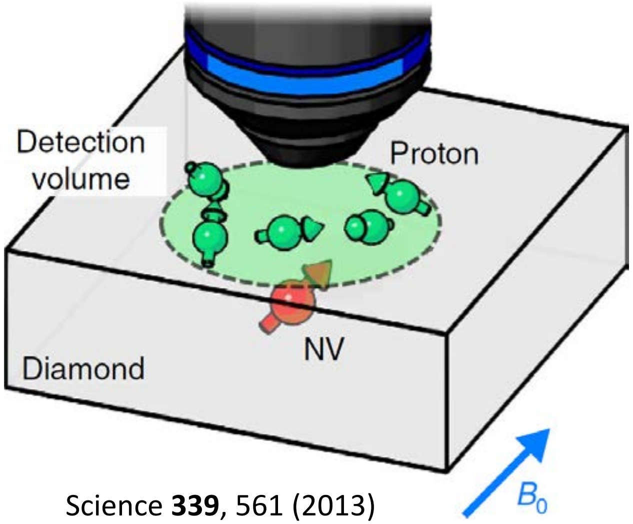

Science **339**, 561 (2013)

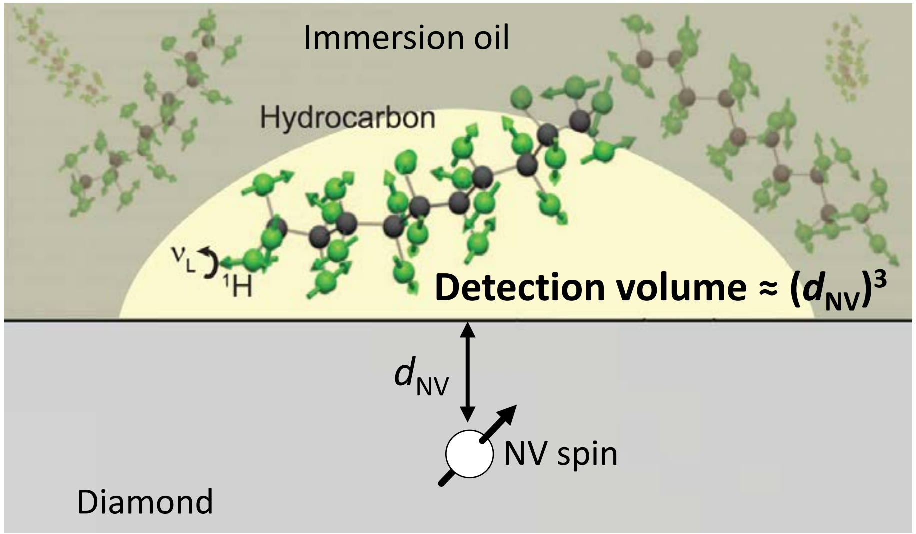

Nature Commun. **6**, 8527 (2015)

Nuclear spins **precess** at f_{ac} = a few kHz–MHz under B_0

⇨ **Weak AC magnetic field** on the NV spin

⇨ Detect using **quantum coherence**

Magnetic resonance

Torque equation (Larmor precession)

$$\frac{d\boldsymbol{\mu}}{dt} = \boldsymbol{\mu} \times \gamma \boldsymbol{B}_0$$

Gyromagnetic ratio

Magnetic moment: $\boldsymbol{\mu} = \gamma \boldsymbol{J}$

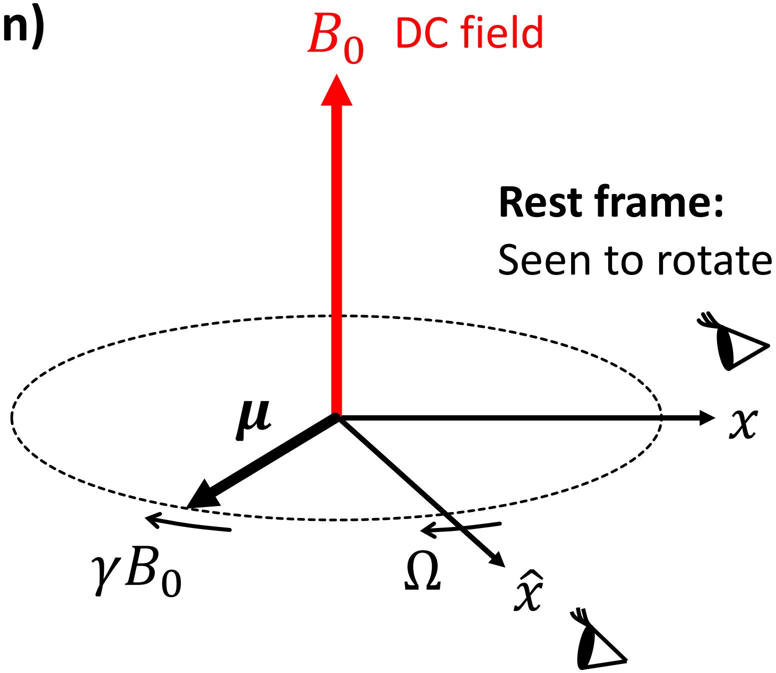

Rest frame:
Seen to rotate at γB_0

Frame rotating at angular velocity Ω:
Rotate slower…why?

Joseph Larmor
(1857–1942)

(from Wikipedia)

Magnetic resonance

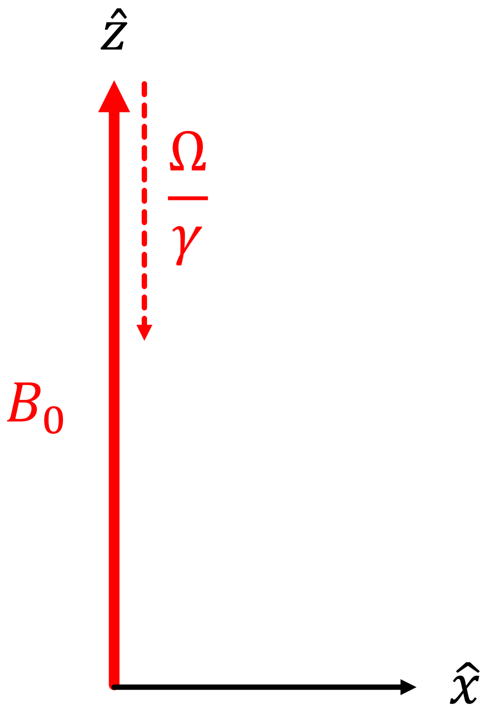

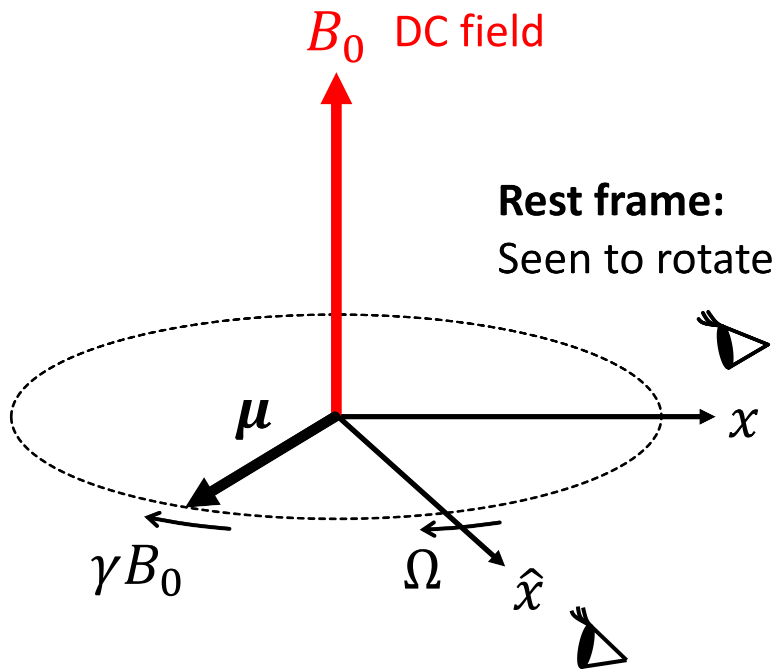

Rest frame:
Seen to rotate at γB_0

Frame rotating at angular velocity Ω:
Rotate slower…why?

⇩

DC field along the z direction becomes weaker

Magnetic resonance

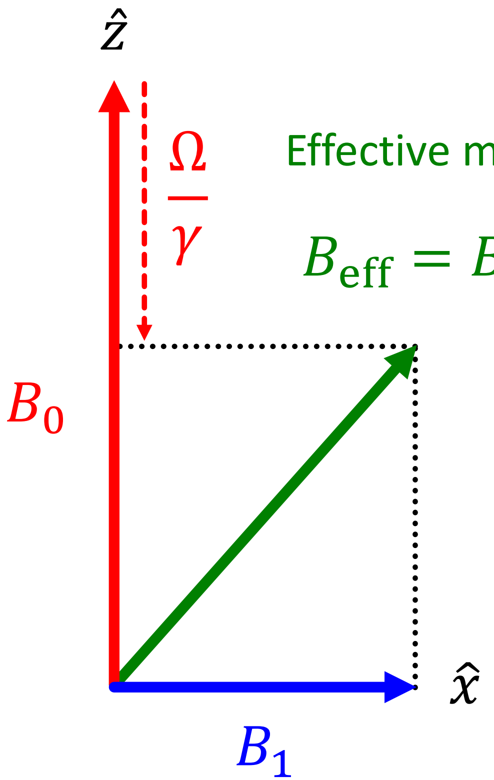

Effective magnetic field

$$B_{\text{eff}} = B_1\hat{x} + \left(B_0 - \frac{\Omega}{\gamma}\right)\hat{z}$$

AC field rotating in the xy plane at Ω

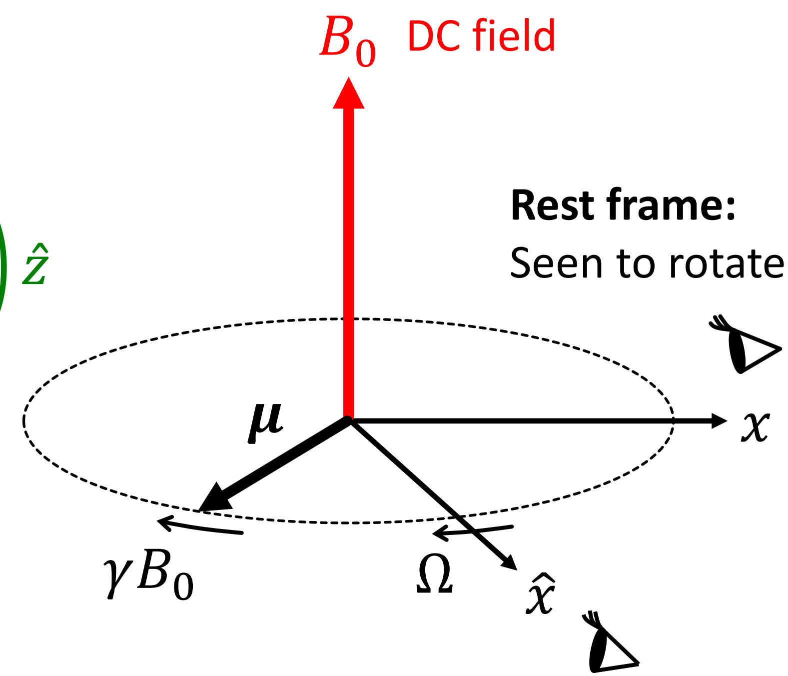

Rest frame:
Seen to rotate at γB_0

Frame rotating at angular velocity Ω:
Rotate slower…why?

DC field along the z direction becomes weaker

Magnetic resonance

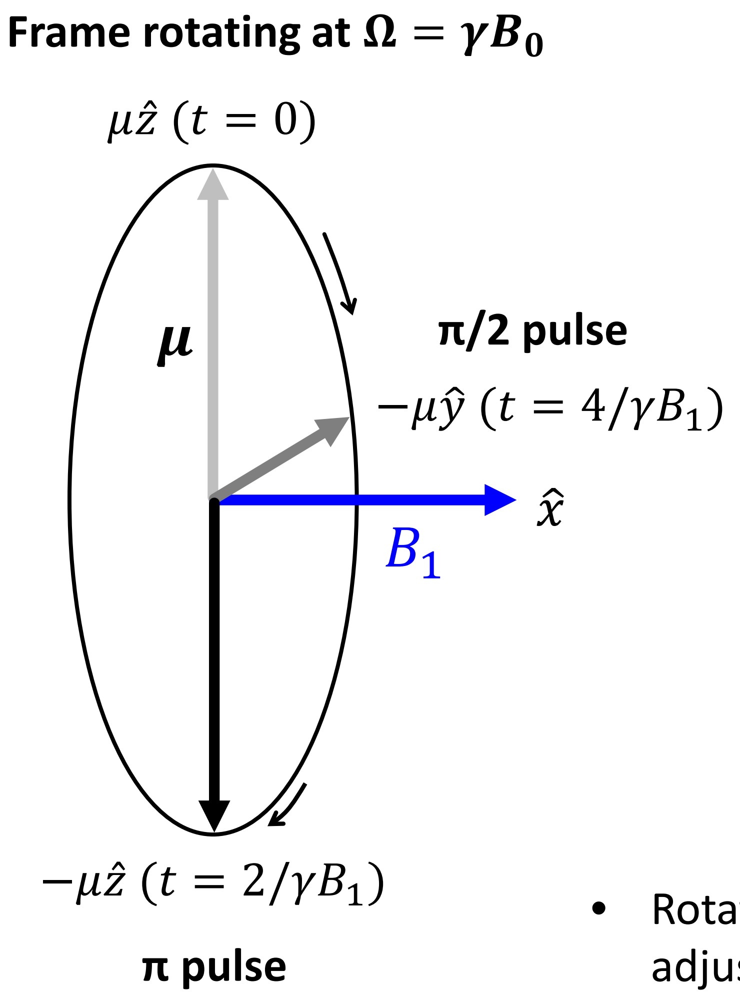

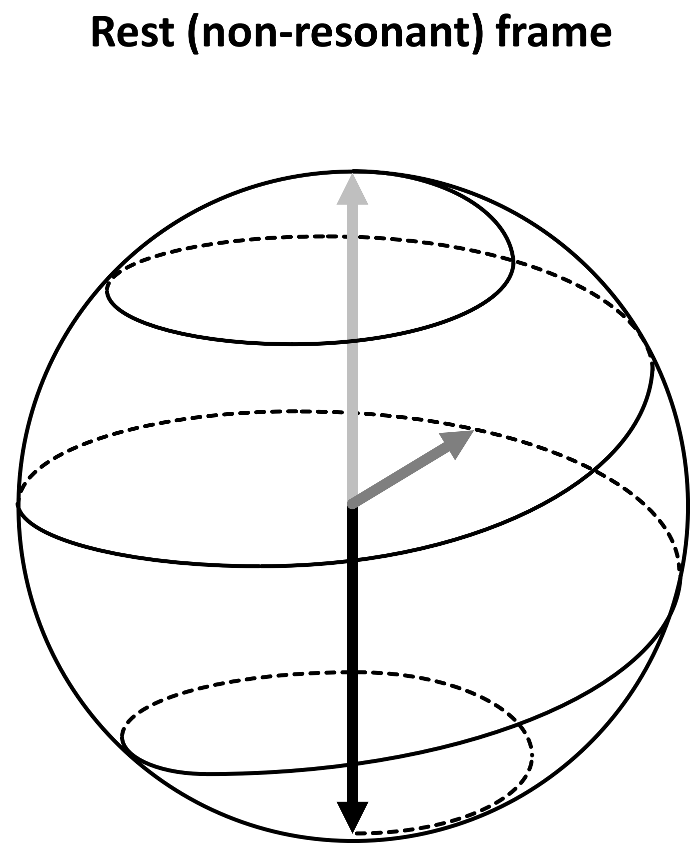

- Rotations about the $\pm\hat{x}, \pm\hat{y}$ axes are realized by adjusting the microwave phases
- Rotation about the $\hat{z}$ axis is superposed when observed from the rest (non-resonant) frame

Quantum bit

Qubit, spin-1/2 (NV is spin-1!)

$$\begin{cases} |"0"\rangle \equiv |m_s = 0\rangle \\ |"1"\rangle \equiv |m_s = -1\rangle \end{cases}$$

Superposition state

$$|\psi\rangle = \alpha|0\rangle + \beta|1\rangle \qquad |\alpha|^2 + |\beta|^2 = 1$$

⇩

$$|\psi\rangle = \underline{e^{i\gamma}}\left(\cos\frac{\theta}{2}|0\rangle + e^{i\phi}\sin\frac{\theta}{2}|1\rangle\right)$$

Global phase

$0 \le \theta \le \pi$

$0 \le \gamma, \phi < 2\pi$

⇩

$$|\psi\rangle = \cos\frac{\theta}{2}|0\rangle + e^{i\phi}\sin\frac{\theta}{2}|1\rangle$$

$0 \le \theta \le \pi$

$0 \le \phi < 2\pi$

Bloch sphere

Qubit, spin-1/2 (NV is spin-1!)

$$\begin{cases} |"0"\rangle \equiv |m_s = 0\rangle \\ |"1"\rangle \equiv |m_s = -1\rangle \end{cases}$$

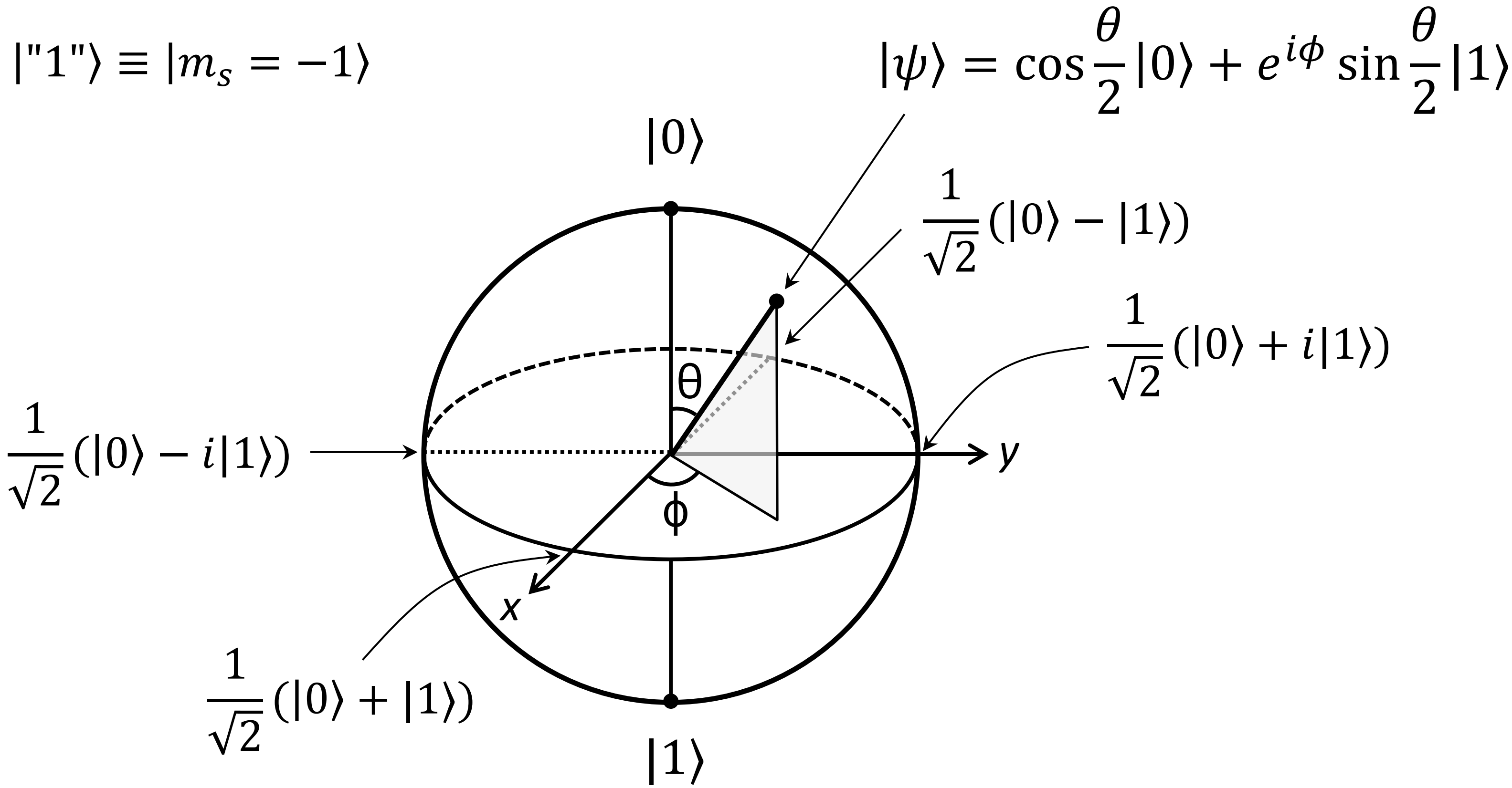

Rabi oscillation

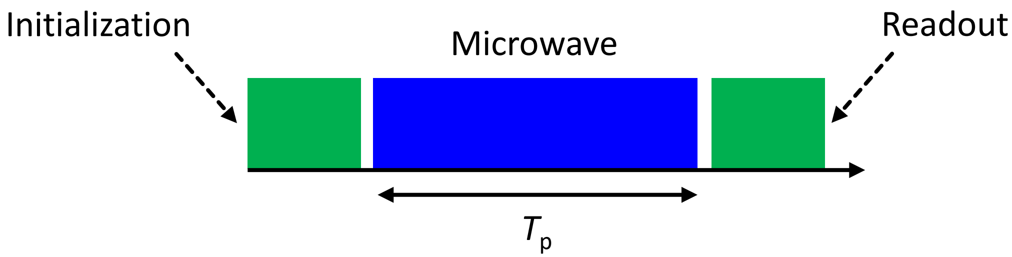

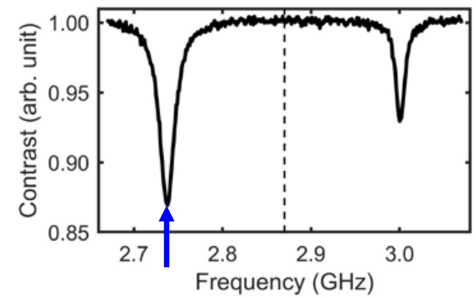

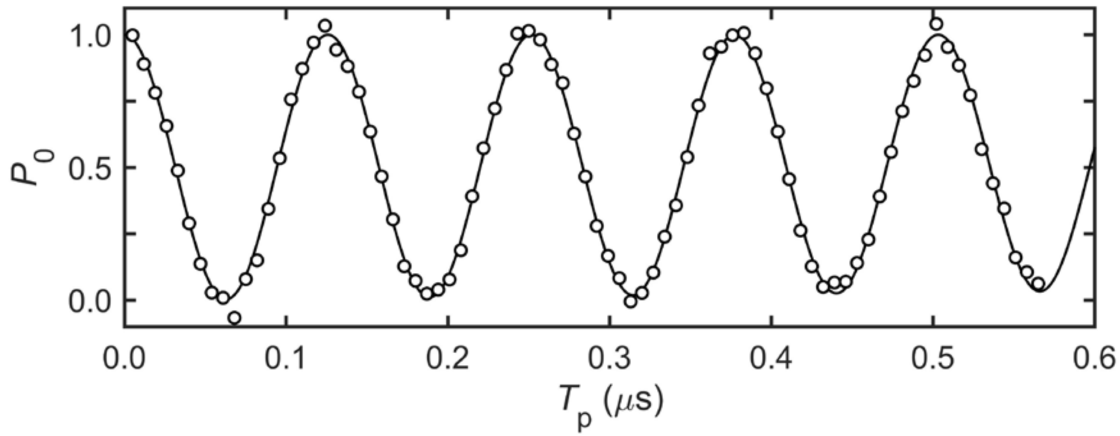

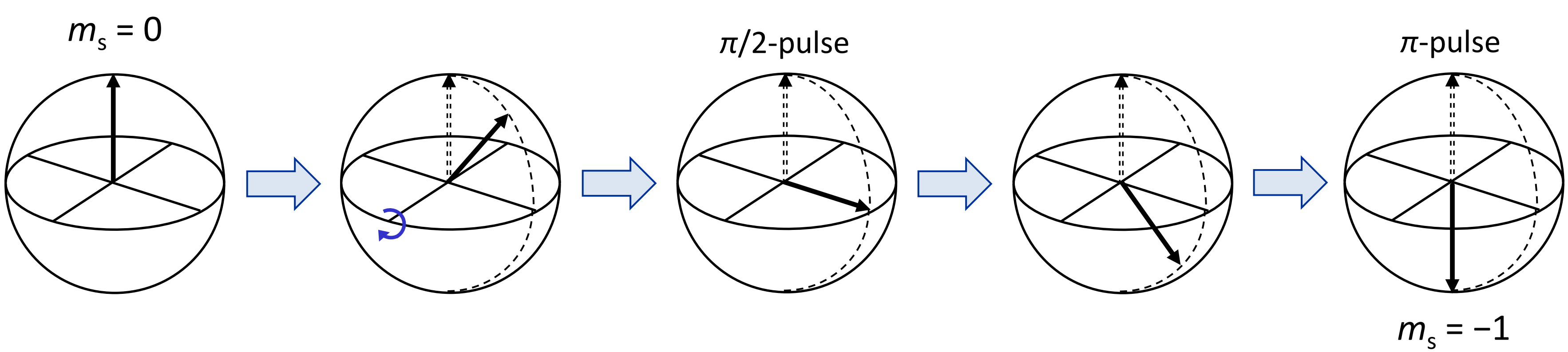

Quantum coherence

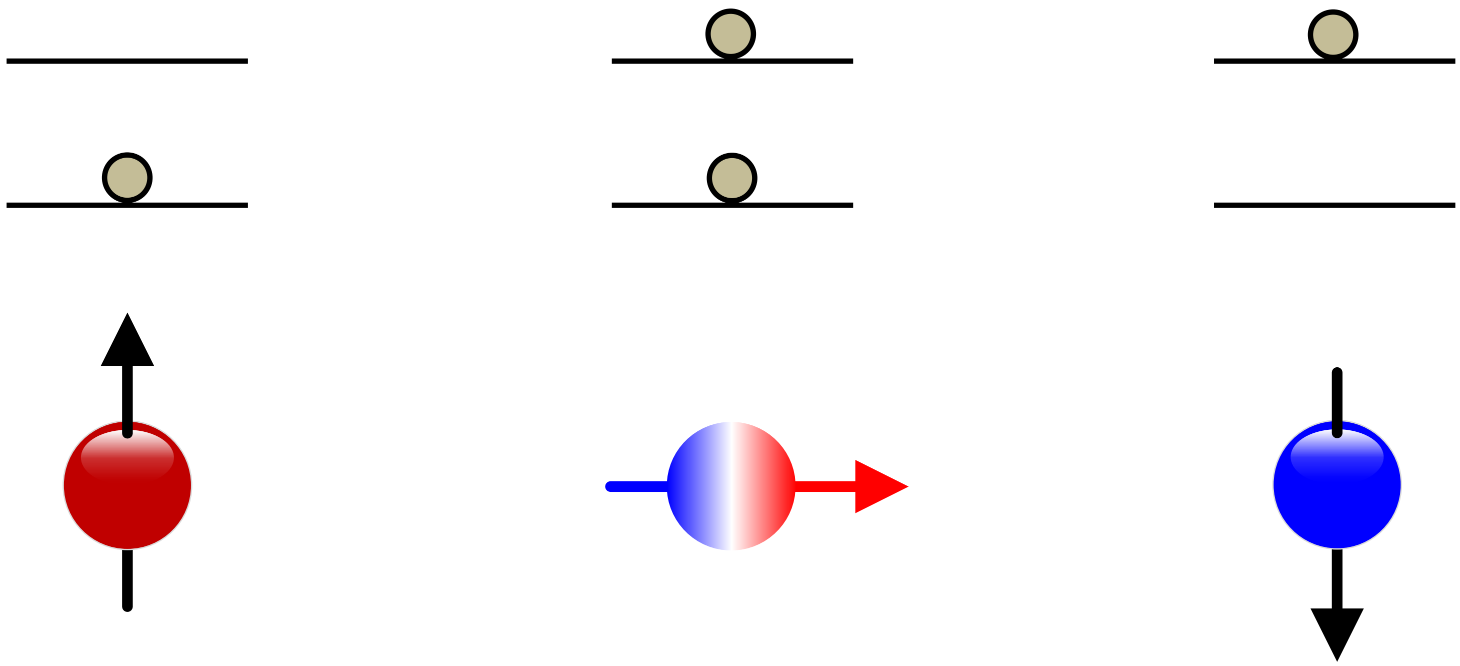

$|0\rangle \equiv |m_s = 0\rangle$ $\quad$ $|\Psi\rangle = \alpha|0\rangle + \beta|1\rangle$ $\quad$ $|1\rangle \equiv |m_s = -1\rangle$

***T_2*: measure of how long a superposition state is preserved**

Measurement of T_2

Time domain → Decay time constant T_2

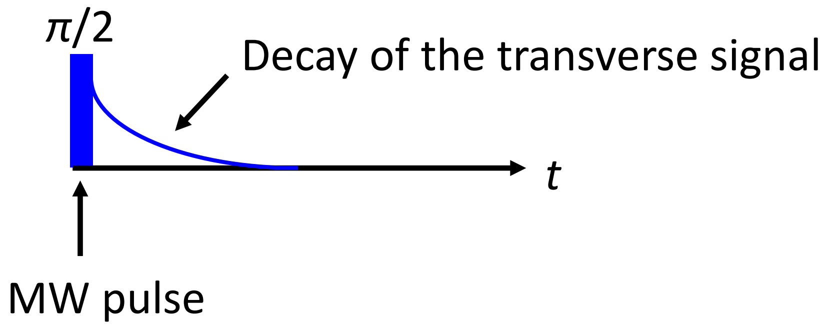

Frequency domain → Lorentz width

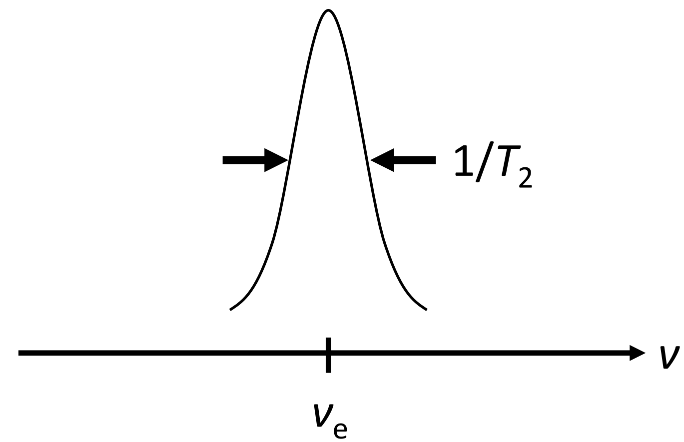

Measurement of T_2

Time domain → Decay time constant T_2

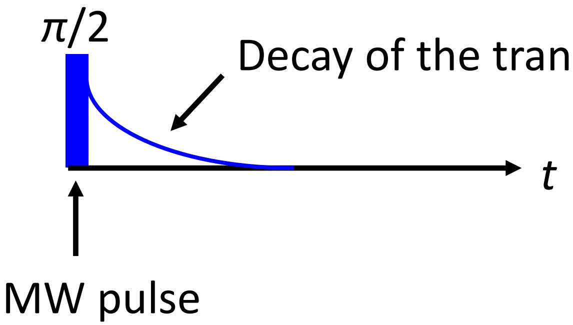

Frequency domain → Lorentz width

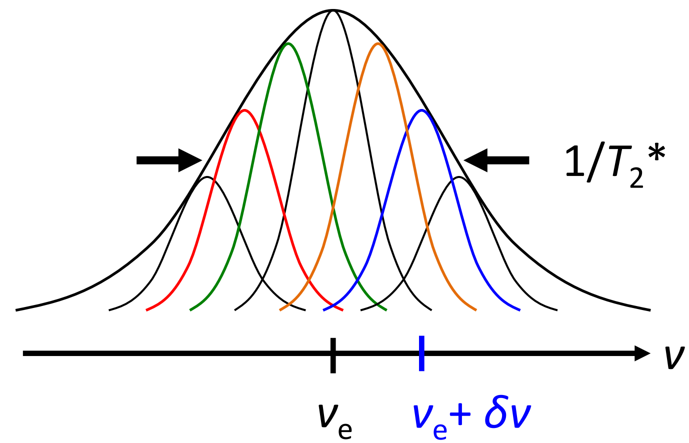

Inhomogeneous line broadening

Seen to precess at $\delta\nu$ in the frame rotating at ν_e

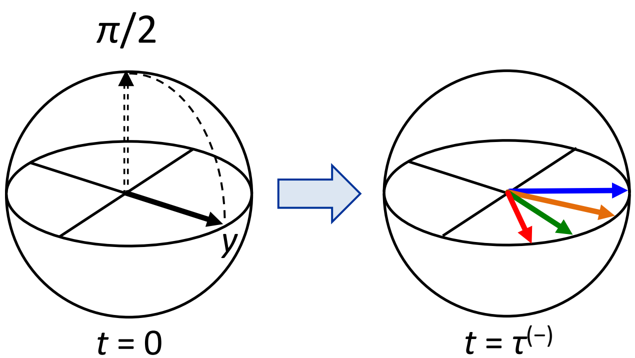

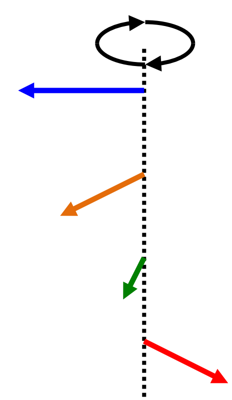

Spin echo

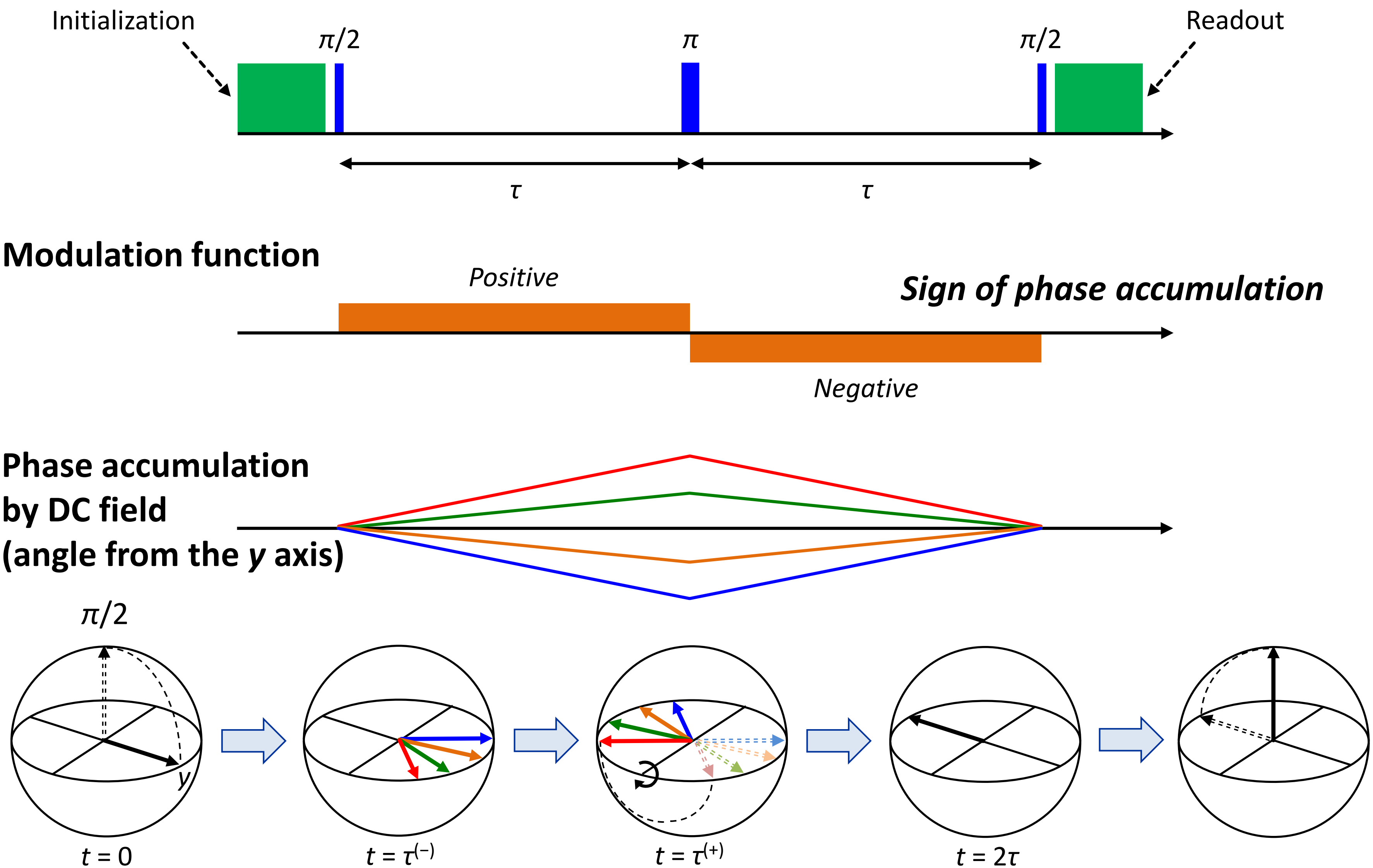
Initialization
π/2
π
π/2
Readout
τ
τ
Modulation function
Positive
Sign of phase accumulation
Negative
Phase accumulation
by DC field
(angle from the y axis)
π/2
y
t = 0
t = τ(−)
t = τ(+)
t = 2τ

Coherence time

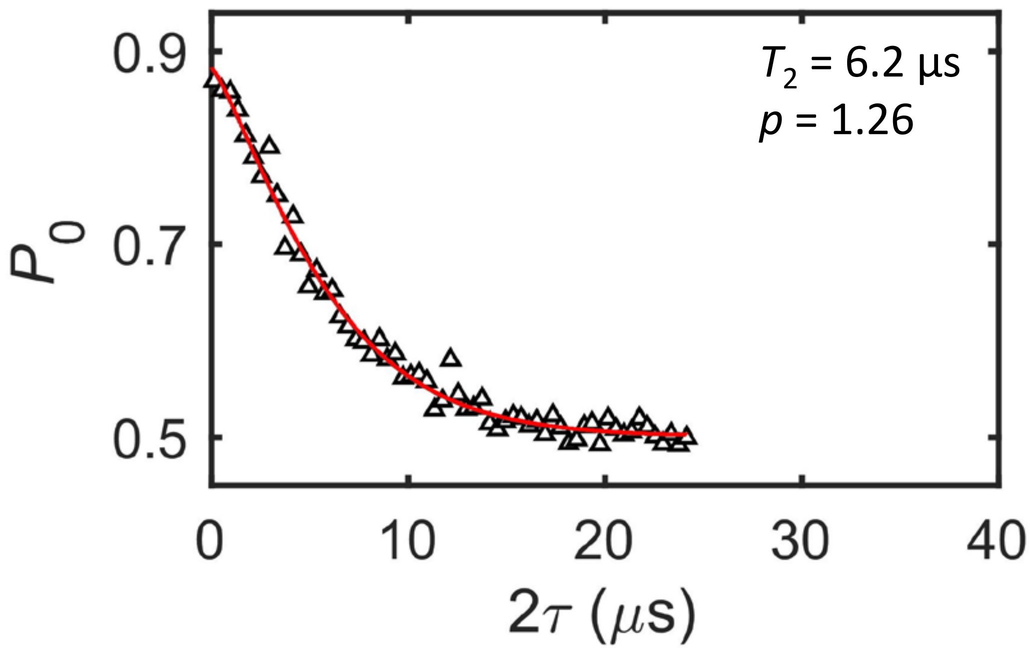

Stretched exponential decay

$$\exp\left[-\left(\frac{2\tau}{T_2}\right)^p\right]$$

Near-surface NV center

- N^+ implantation into ^{12}C (I = 0) layer
- d_{NV} = 6.26 nm
- B_0 = 23.5 mT

AIP Advances **10**, 025206 (2020) Misonou *et al.*

AC magnetometry

CP (N = 4)

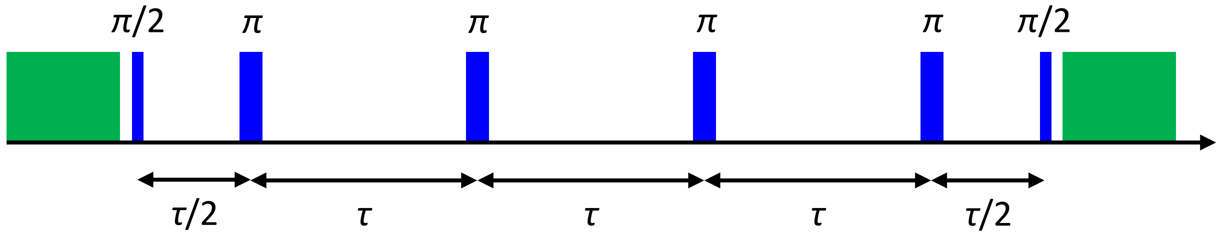

Modulation function

AC field at f_{ac} = 1/2τ

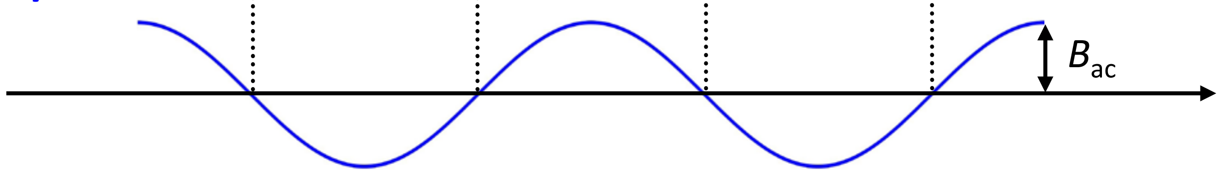

Sensor phase buildup = loss of coherence

$$\gamma B_{\mathrm{ac}} \int_0^t |\cos(2\pi f_{\mathrm{ac}} t)|\, dt$$

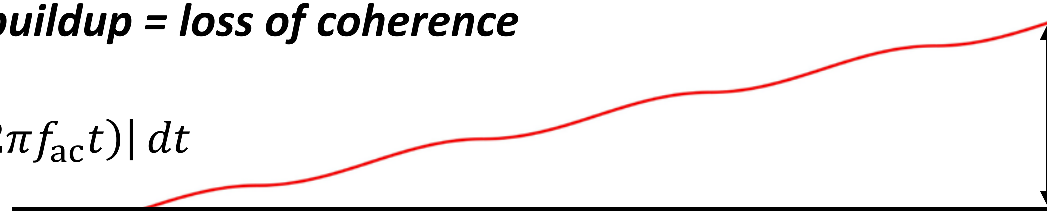

Nuclear spin sensing

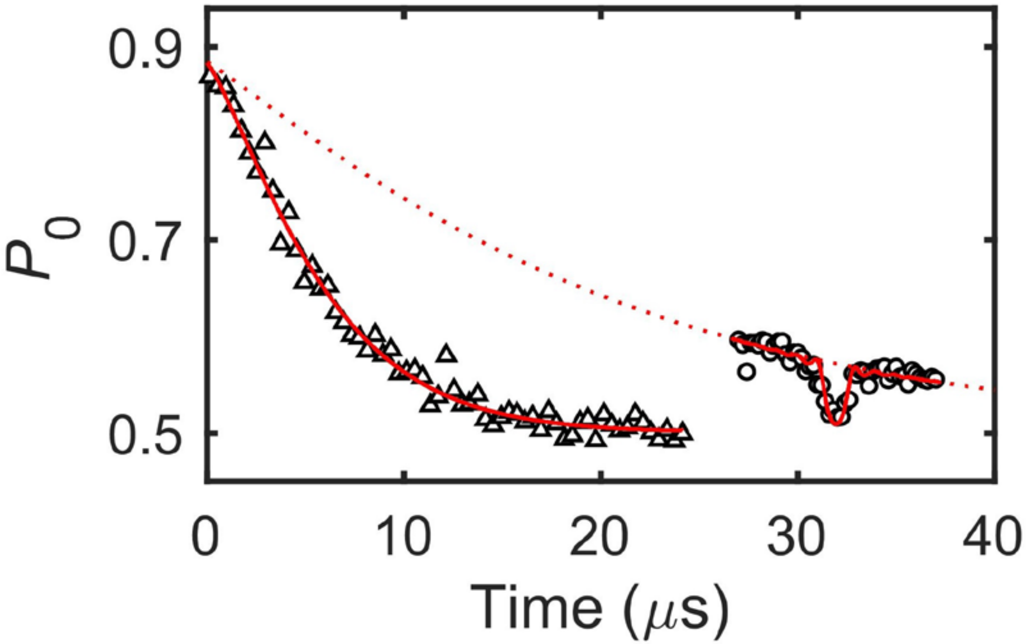

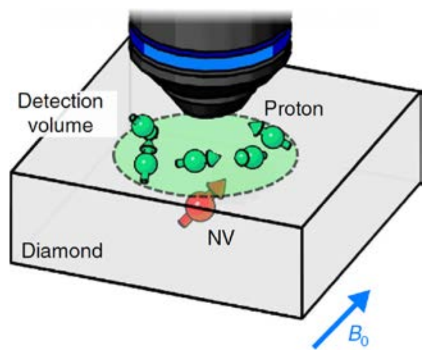

- T_2 = 6.2 μs @B_0 = 23.5 mT
- N = 64 (XY16)
- $(2\tau)^{-1}$ = 64/(2 x 32 μs) = 1 μs
  → $\gamma_H B_0$ = (42.577 kHz/mT) x B_0 = 1.00 MHz

AIP Advances **10**, 025206 (2020) Misonou *et al.*

Nuclear spin sensing

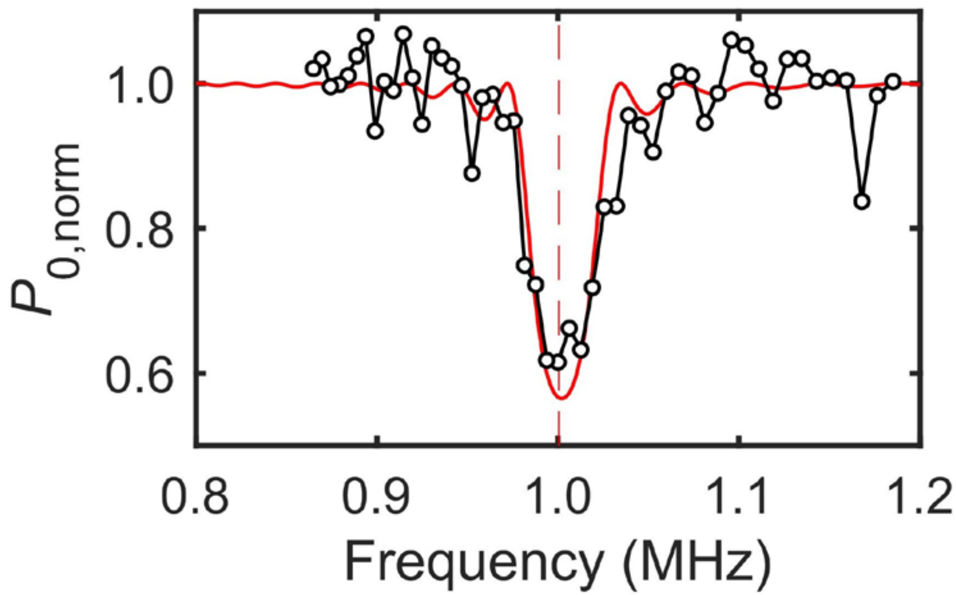

$$C(\tau) = f(B_{\mathrm{rms}})$$

$$B_{\mathrm{rms}} = \frac{\mu_0}{4\pi} h\gamma_{\mathrm{H}} \sqrt{\frac{5\pi\rho}{96 d_{\mathrm{NV}}^3}}$$

Phys. Rev. B **93**, 045425 (2016)

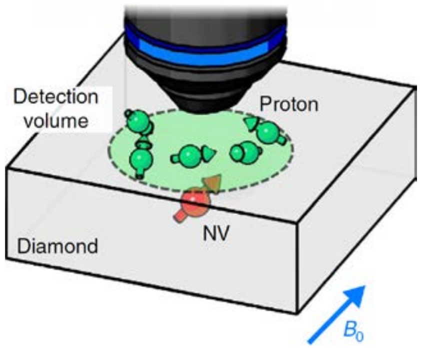

- Proton density ρ = 6 x 10^{28} m^{-3} (known)
- d_{NV} = 6.26 nm
- B_{rms} ≈ 560 nT
- Detection volume $(d_{\mathrm{NV}})^3$ ≈ 0.25 zL (zepto = 10^{-21})
- # of proton $\rho(d_{\mathrm{NV}})^3$ ≈ 1500
- Thermal pol. (10^{-7}) vs. statistical pol. $(1500)^{0.5}$ ≈ 39

AIP Advances **10**, 025206 (2020) Misonou *et al.*

Toward single-molecular imaging

- **Spectral resolution**
  → Easy to resolve isotopes
  → Need to measure *J*-couplings & chemical shifts (ppm!)
  → Limited by sensor/memory lifetimes ($T_{2e/n}$, $T_{1e/n}$)

- **Information of the positions of the individual nuclei**
  → Accurate measurement of *e*–*n* int. const's ($A_{\parallel}$, $A_{\perp}$) ≈ (r, θ)
  → Lack of information on the azimuthal angle ϕ

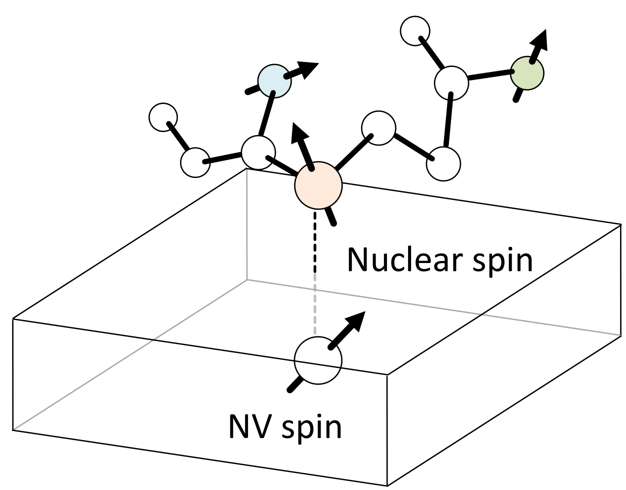

Toward single-molecular imaging

- **Spectral resolution**
  → Easy to resolve isotopes
  → Need to measure *J*-couplings & chemical shifts (ppm!)
  → Limited by sensor/memory lifetimes ($T_{2e/n}$, $T_{1e/n}$)

- **Information of the positions of the individual nuclei**
  → Accurate measurement of *e*–*n* int. const's ($A_{\parallel}$, $A_{\perp}$) ≈ (r, θ)
  → Lack of information on the azimuthal angle ϕ

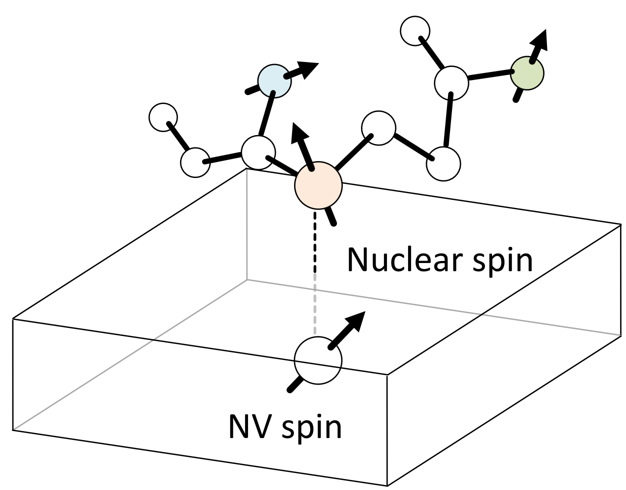

AC magnetometry

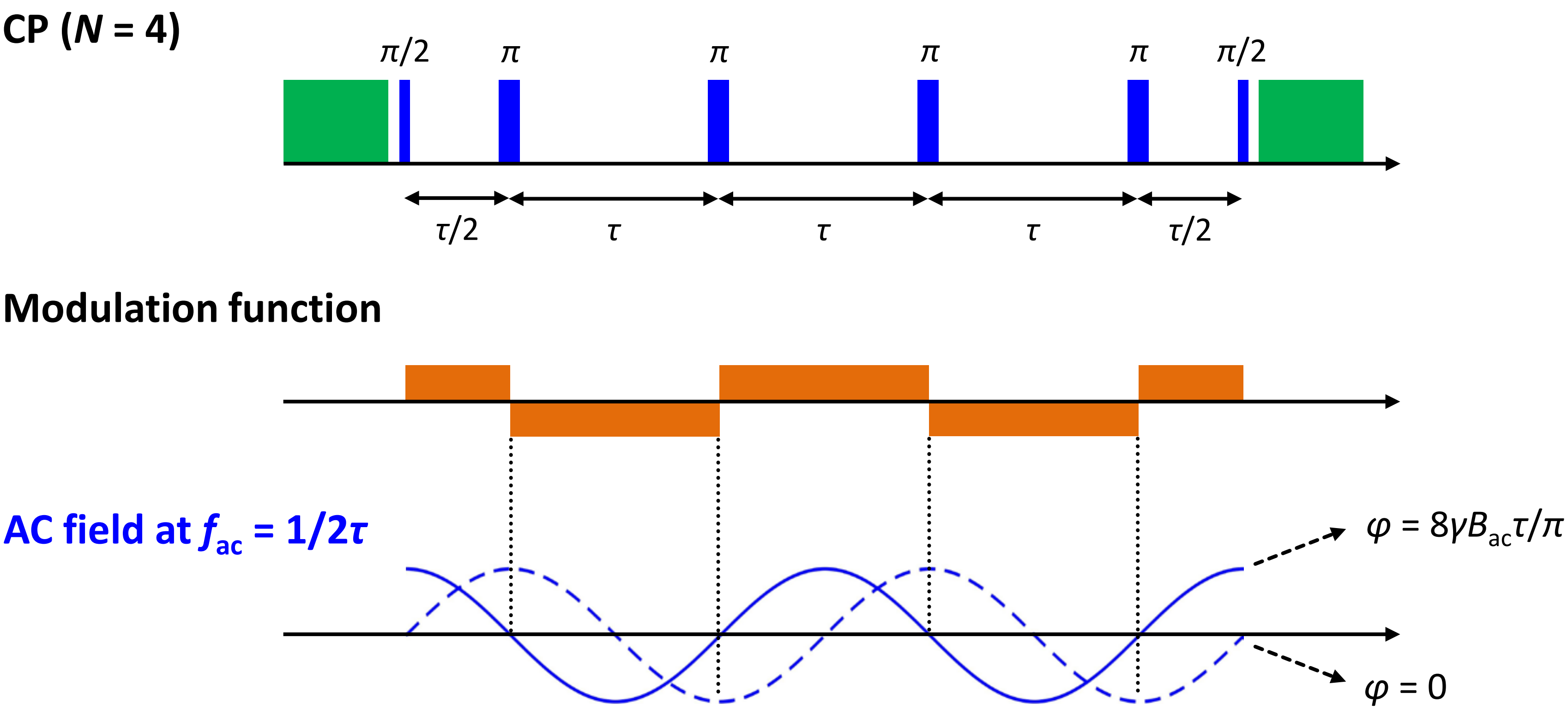

- φ depends on the **initial phase $\boldsymbol{\alpha}$ of the AC field** ($\varphi \propto \cos \alpha$)

AC magnetometry

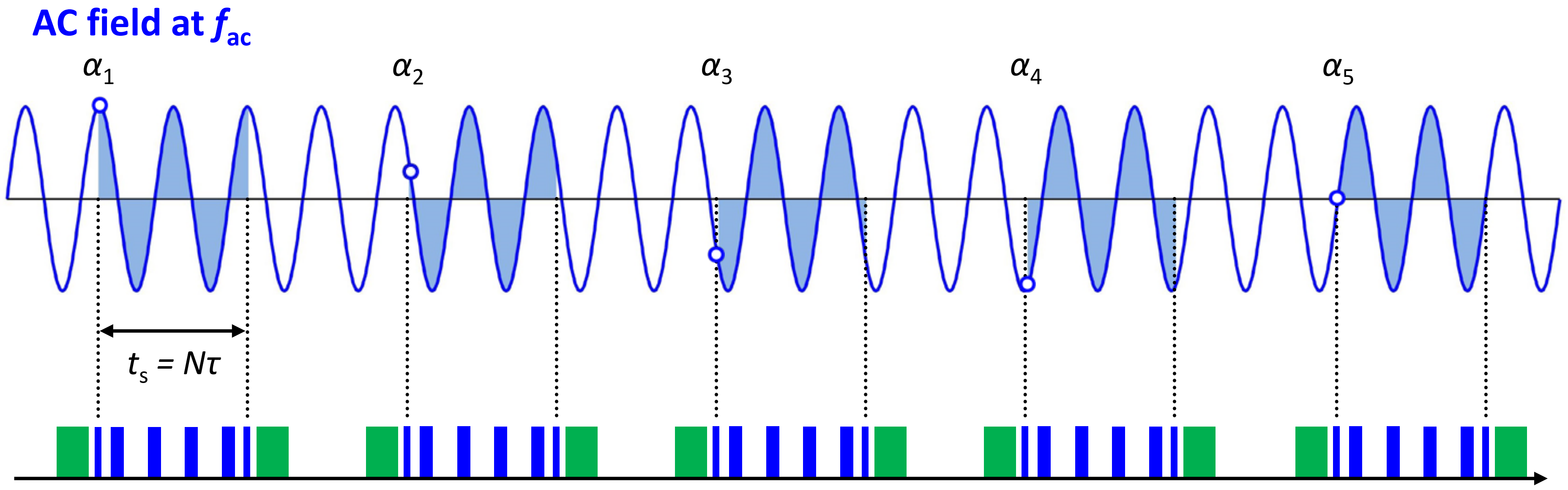

- φ depends on the **initial phase $\boldsymbol{\alpha}$ of the AC field** ($\varphi \propto \cos \alpha$)
- Average over **random $\boldsymbol{\alpha}$**

Ultrahigh resolution sensing

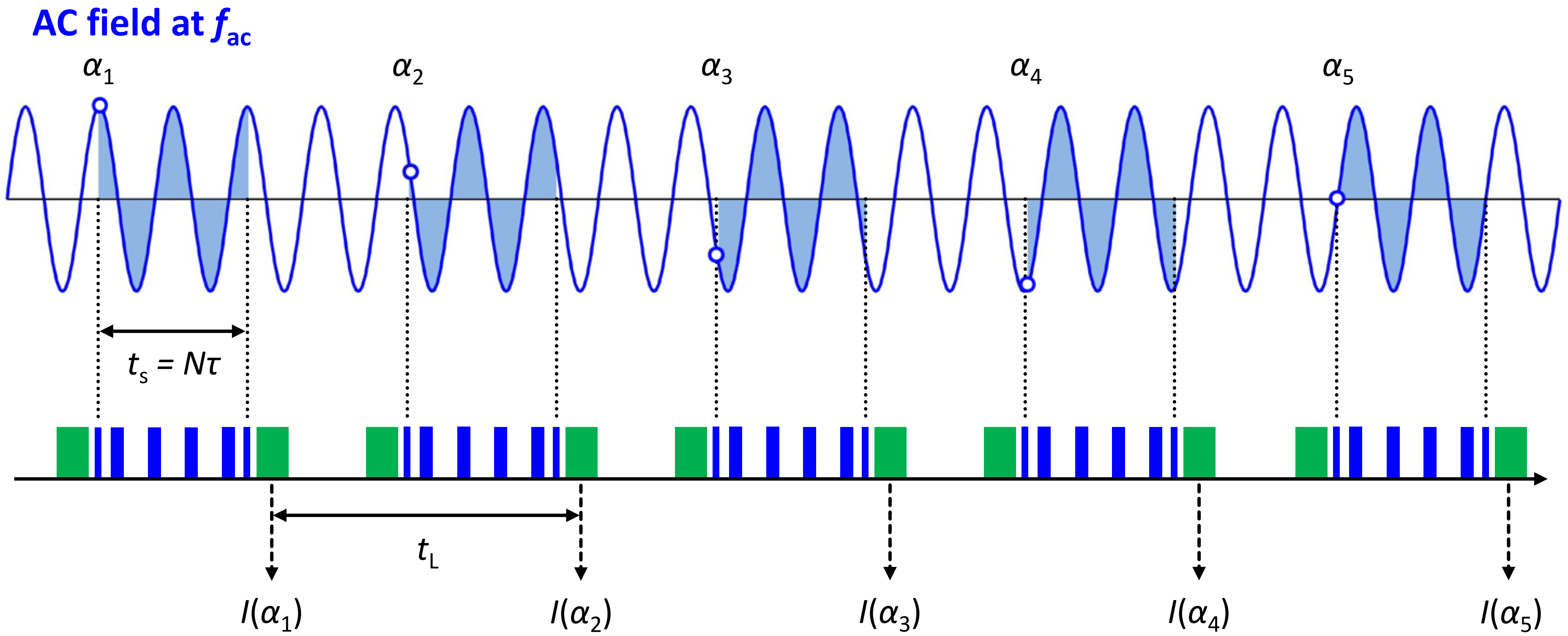

- φ depends on the **initial phase $\boldsymbol{\alpha}$ of the AC field** ($\varphi \propto \cos\alpha$)
- Average over **random $\boldsymbol{\alpha}$**
- **If the data acq. is periodic,** adjacent α's are related by $\alpha_{k+1} = 2\pi f_{ac} t_L + \alpha_k$

Science **356**, 832 (2017) Schmitt *et al.*; Science **356**, 837 (2017) Boss *et al.*; Nature **555**, 351 (2018) Glenn *et al.*

Ultrahigh resolution sensing

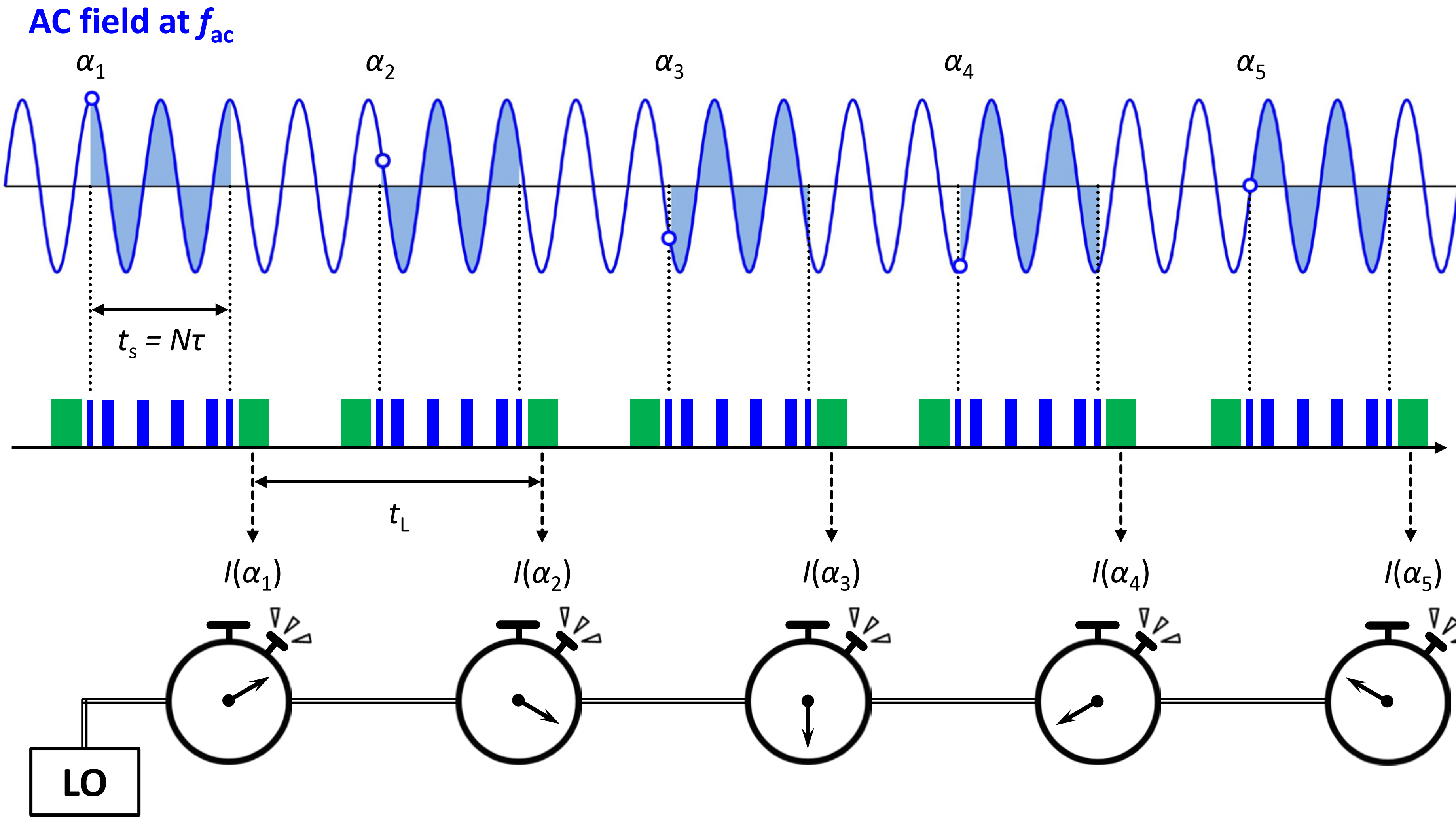

Science **356**, 832 (2017) Schmitt *et al.*; Science **356**, 837 (2017) Boss *et al.*; Nature **555**, 351 (2018) Glenn *et al.*

Ultrahigh resolution sensing

B_{ac} = 96.5 nT & f_{ac} = 2.001 MHz applied from a coil, detected by a single NV center

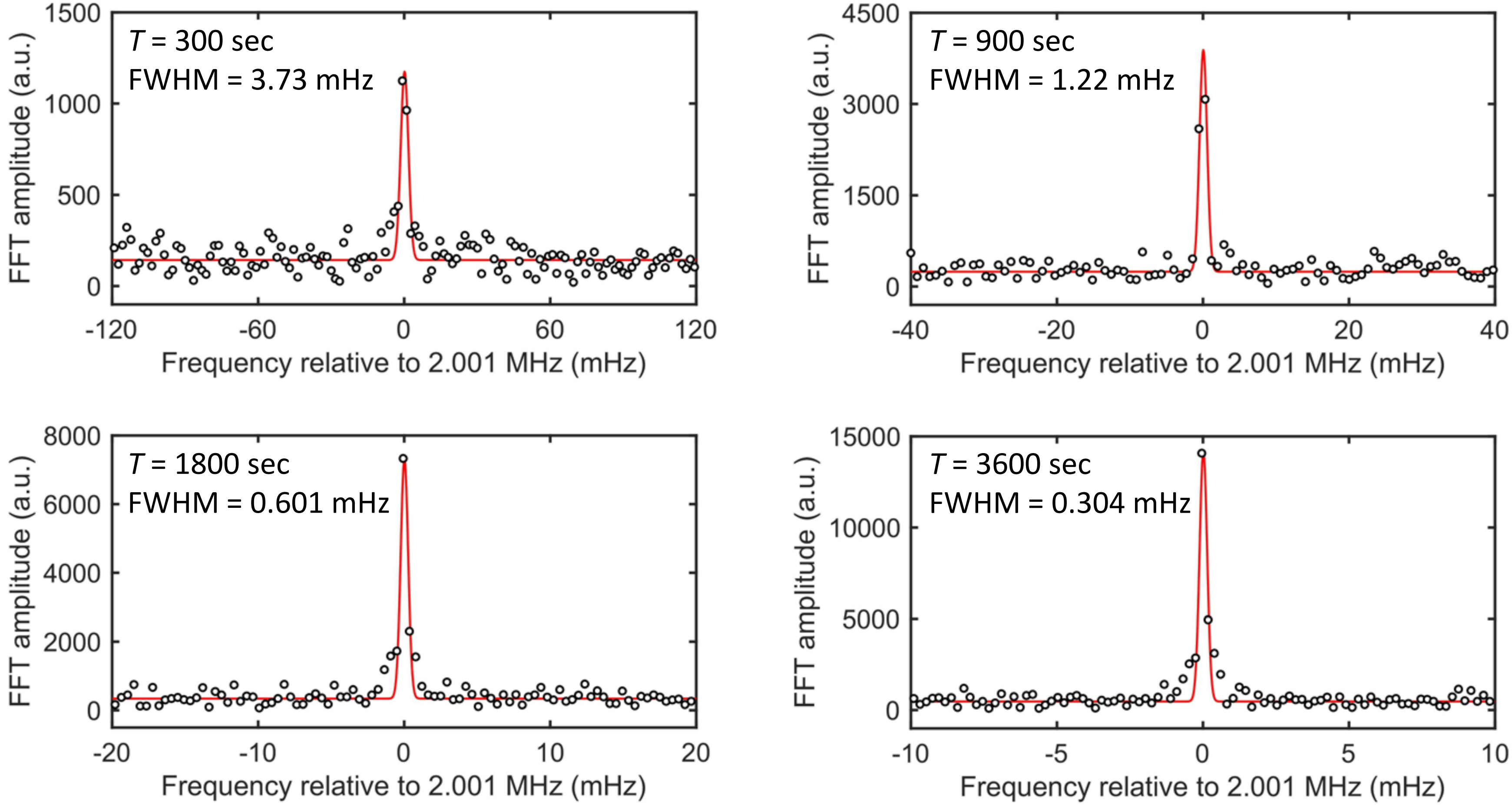

J. Appl. Phys. **123**, 161101 (2018) Abe & Sasaki

Ultrahigh resolution sensing

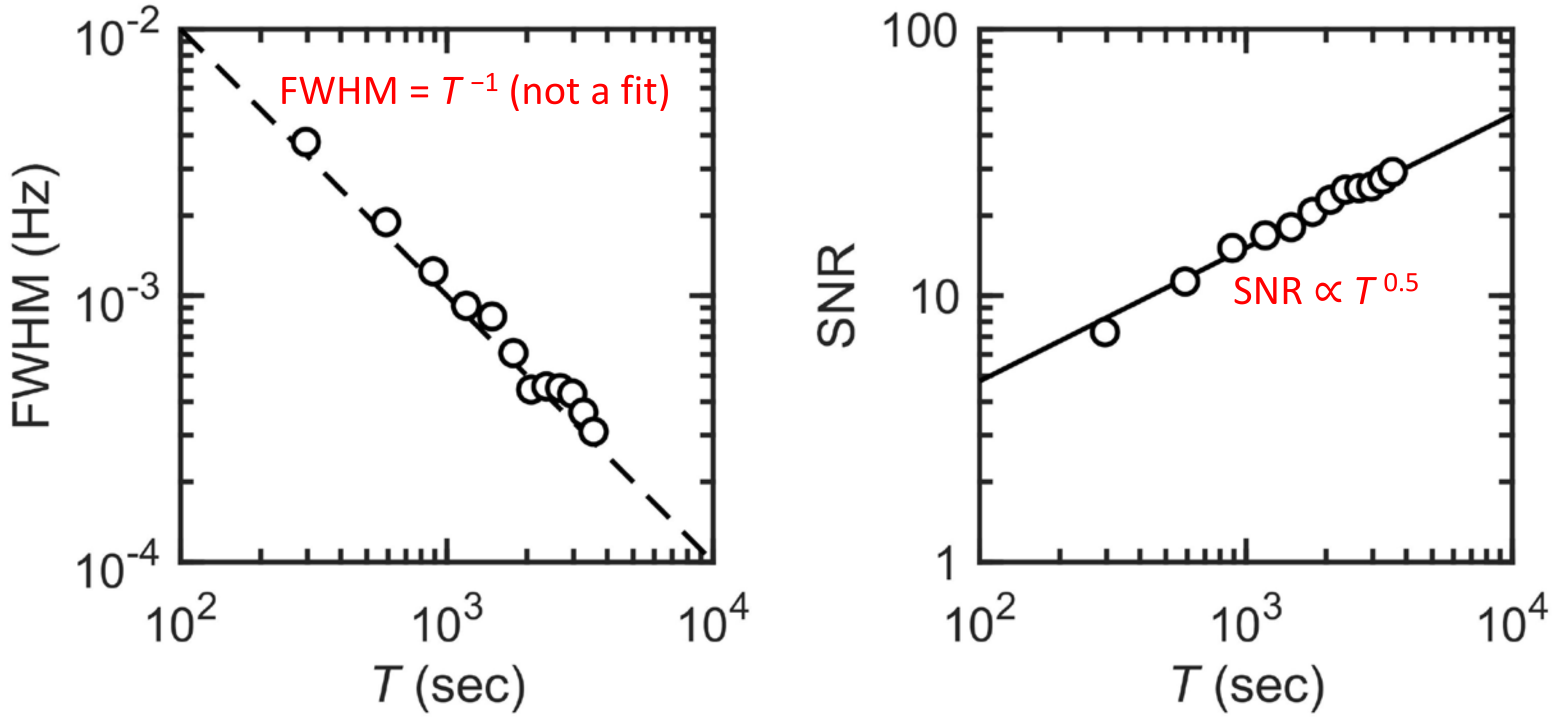

- Spectral resolution not limited by sensor/memory lifetimes ($T_{2e/n}$, $T_{1e/n}$)
- Only limited by the stability of LO (essentially infinite)
- Resolution = T^{-1} & SNR ∝ $T^{0.5}$ → Precision ∝ $T^{-1.5}$

J. Appl. Phys. **123**, 161101 (2018) Abe & Sasaki

NMR spectroscopy

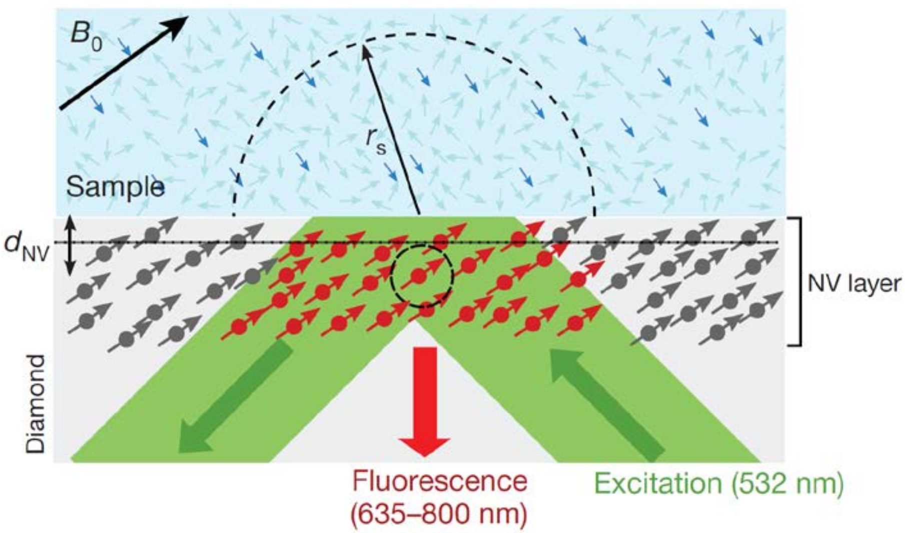

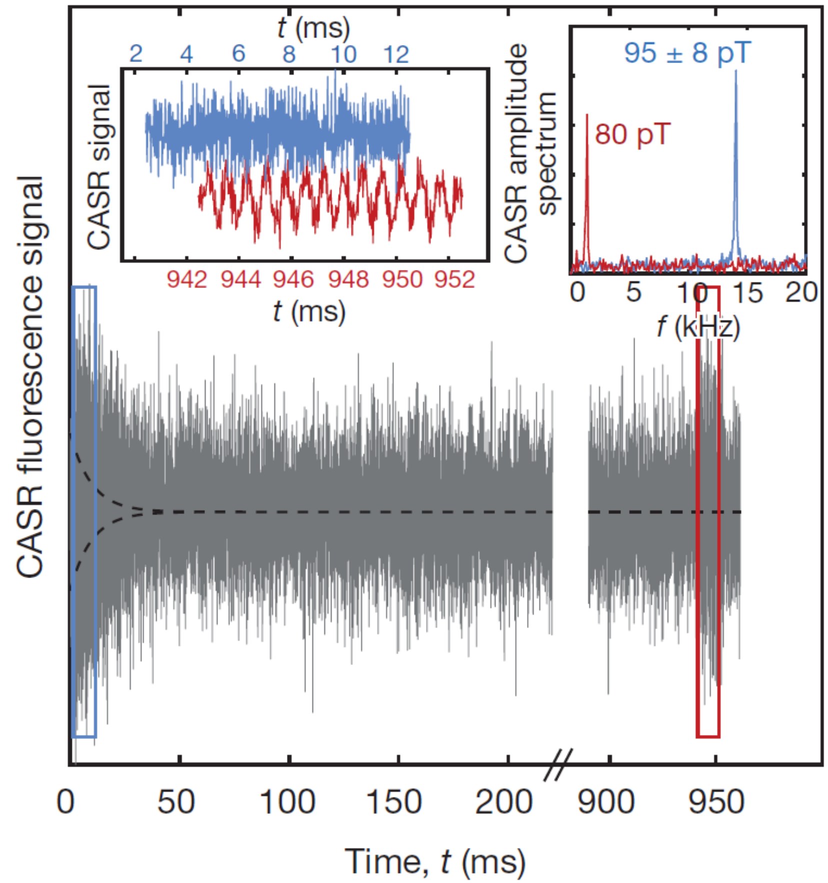

- $[NV] \approx 3 \times 10^{17}$ cm^{-3}
- # of NV ≈ 5×10^9
- $V_{detect} \approx 25$ pL
- # of protons ≈ 2.5×10^{15}
- RF pulse → FID

See also: Science **357**, 67 (2017) Aslam *et al.* [B_0 = 3 T, f_e = 87 GHz, T_{1n} = 260 s]

Nature **555**, 351 (2018) Glenn *et al.*

NMR spectroscopy

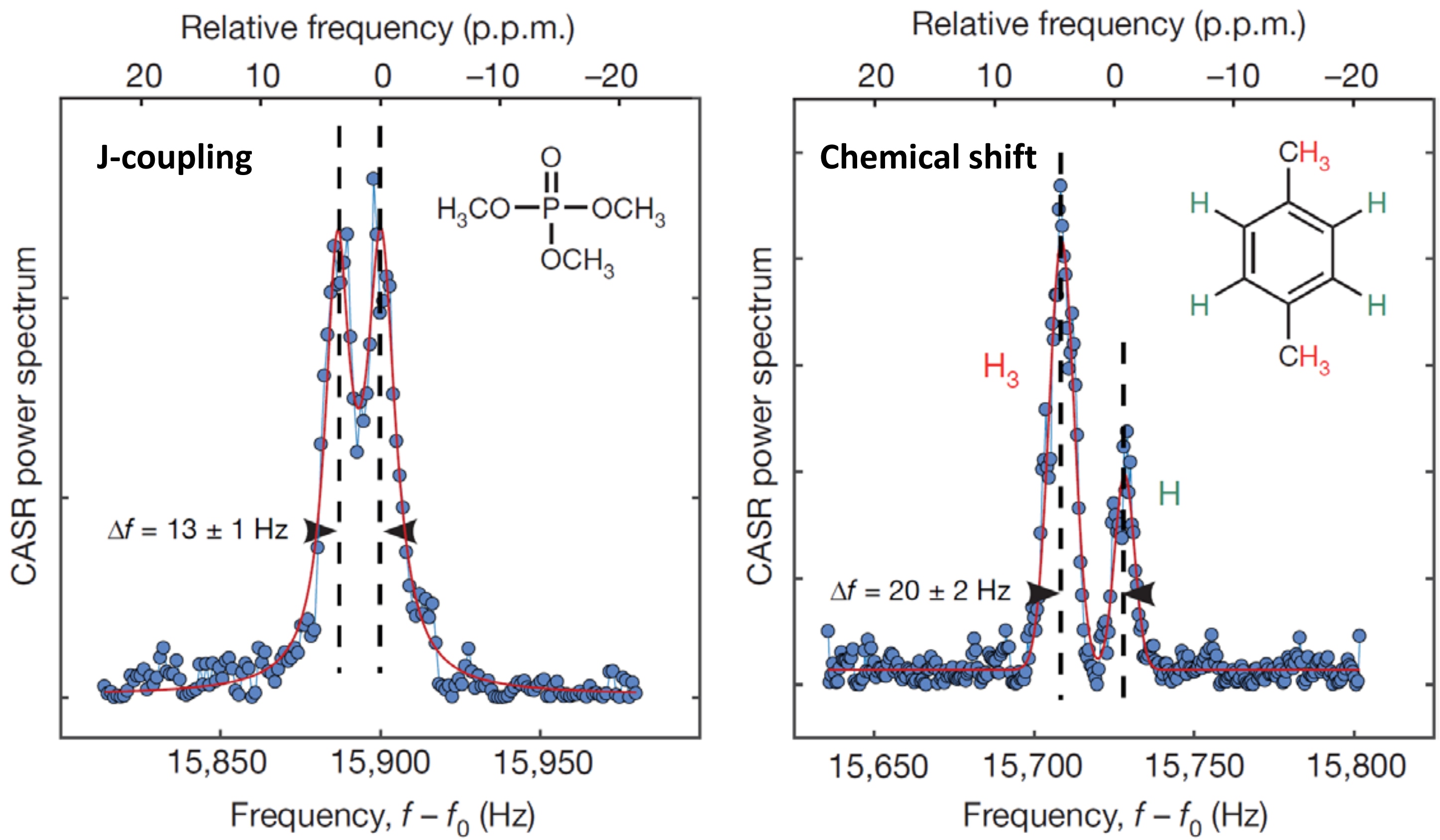

See also: Science **357**, 67 (2017) Aslam *et al.* [B_0 = 3 T, f_e = 87 GHz, T_{1n} = 260 s]

Nature **555**, 351 (2018) Glenn *et al.*

Toward single-molecular imaging

- **Spectral resolution**
  → Easy to resolve isotopes
  → Need to measure *J*-couplings & chemical shifts (ppm!)
  → Limited by sensor/memory lifetimes ($T_{2e/n}$, $T_{1e/n}$)

- **Information of the positions of the individual nuclei**
  → Accurate measurement of *e*–*n* int. const's ($A_{\parallel}$, $A_{\perp}$) ≈ (r, θ)
  → Lack of information on the azimuthal angle ϕ

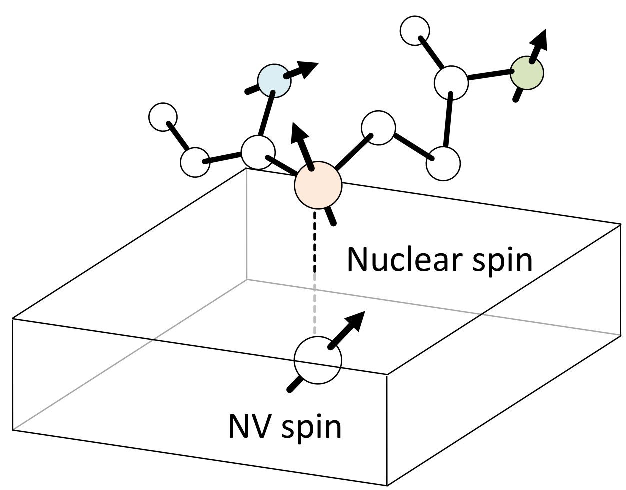

Summary

- **Applications to biology, geoscience, condensed matter...**

- **Tools for single-molecule imaging/structural analysis are being developed**
  → Ultrahigh resolution sensing[1,2,3], resolving chemical shifts[3,4] & suppression of back action from *n*-spins[5,6]
  → Determination of the position of individual *n*-spins[7,8,9]

[1] Science **356**, 832 (2017) Schmitt *et al.* (Ulm)
[2] Science **356**, 837 (2017) Boss *et al.* (ETH)
[3] Nature **555**, 351 (2018) Glenn *et al.* (Harvard)
[4] Science **357**, 67 (2017) Aslam *et al.* (Stuttgart)
[5] Nature Commun. **10**, 594 (2019) Pfender *et al.* (Stuttgart)
[6] Nature **571**, 230 (2019) Cujia *et al.* (ETH)
[7] Phys. Rev. B **98**, 121405 (2018) Sasaki *et al.* (Keio)
[8] Phys. Rev. Lett. **121**, 170801 (2018) Zopes *et al.* (ETH)
[9] Nature **576**, 411 (2019) Abobeih *et al.* (Delft)